Institute of Space and Aeronautical Science, University of Tokyo
Report No. 482, June 1972

"A Fundamental Study on Safe Landing"

By

Akira OBATA*

Summary: It is ascertained that reachable or controllable points of a dynamic system in which a system equation is linear with respect to control variables can be obtained even for cases with first-order state-inequality-constraint by using an effective optimizing method based on linear programming.

With this method, controllable height regions of aircraft for spot landing are investigated. The effect of flight parameters such as approach path angle and velocity and the effects of the constraint quantities of elevator angle, angle of attack and pitch attitude on the controllable region are made clear for a middle size turbo-prop transport aircraft.

The widest controllable height region of the model aircraft at 1/3 naut mile point from landing spot is obtained at the approach velocity of $1.125 \sim 1.175\ V_s$ irrespective of approach angle.

A safety margin factor which is the ratio of maximum allowable steady flight length to the total approach and landing flight length in statistical meanings is introduced and effects of the approach speeds and angles to this factor are discussed.

It may be concluded that the slope of the glide path of the conventional aircraft ($-2.5 \sim -3.0$ deg.) in ILS is reasonable in view of safety and that, if selected carefully, the location of this glide path to an objectvie touch down point can be held to the specified point without any adjustment due to the degree of skillfulness of the pilot. This adjustment seems to be required for more shallow approach path angle.

NOTATION

a: lift slope
a_{ij}: element of coefficient matrix A
b_{ij}: element of coefficient matrix B
c: vector specifying performance index
$\bar{c}$: mean aerodynamic chord
e: vector specifying final state
f: function of x, u
g: state constraint,
gravity acceleration
$g_{(\alpha)}$: constraint for angle of attack
$\boldsymbol{h}$: height (m)
h: non-dim. height ($2\boldsymbol{h}/\bar{c}$)

* Kawasaki Heavy Industries, Ltd. Gifu Works (In-Service Training Course for Engineers and Researchers at Graduation Lebel).

s: number of blocks of variational control
t: time (sec)
$\hat{t}$: non-dim. time (t/τ)
$t_{pi}, t_q, t_{i\pm}$: time at $pi, q, i\pm$
t_s: safety margin expressed by time
dt, dT: small variation of t, T
u: m dim. control vector
u_i: i-th transformed control vector
$u_{i\pm}$: control at $i+$ or $i-$
v: n dim. control vector
v_i: n dim. control vector
x: n dim. state vector
x_i: i-th element of x
x^0: performance index
dx, dx_i, dx^0: small variation of x, x_i, x^0
A: coefficient matrix of equation of motion
B: coefficient matrix of equation of motion
C: function giving controllable region, or matrix specifying final state
D: matrix specifying final state
I: identity matrix
L: lift
M: terminal manifold
M_{s1}, M_s: safety margin factor
P: matrix constraining state
R: reachable region, or distance to touch down point
S: wing area
U: approach velocity
V_s: stall velocity
W: aircraft gross weight
C_L: lift coefficient
α_0: reference angle of attack
α: angle of attack
$'\alpha$: variational angle of attack
$\alpha_{\max}$: stall angle of attack
γ_0: reference approach angle
γ: approach angle
δ_e: variational elevator angle
θ: variational pitch attitude
Θ: pitch attitude of aircraft
ζ: damping ratio
ρ: air density
ω_n: undamped natural frequency

σ_h^2: variance of height
σ_γ^2: variance of approach angle
τ: time $(\bar{c}/2U)$
$\phi(\tau, t), \varphi$: transition matrix
ψ: discrepancy from final condition
Ψ, ϕ_i: adjoint vector
$\mathscr{H}$: Hamiltonian
$\mathscr{U}$: set of u
$(\cdot)$: differentiation with respect to time
$(\ )'$: transpose matrix or vector
$(\ )^{-1}$: inverse matrix
$(\ )_m$: mean value
$(\ )_N$: reference state
$(\ )_{\max,\min}$: maximum and minimum value
$(\ )_0$: initial or reference state
$(\ )_f$: final state

I. Introduction

The study of safety or reliability of aircraft seems to become more important than before, because even a small accident in flight means loss of large human life for the super sized aircraft such as Boing 747.

Contingent fatal accidents had followed one after another in the sky of Japan in 1966 and such terrible and gigantic scale accidents had never been experienced except in war. In these accidents, the one in landing phase whose cause is presumed as pilot miss means by a tacit consent that the study of aircraft operations or pilot's maneuvers is very important.

If we consider an operation of transport aircraft, the flight phase can be partitioned into three phases such as take-off, cruise and landing. From the view point of the control, the landing phase is conspicious in the sense that the aircraft must be controlled to a specified narrow region or point.

In this paper, allowable region of approach height and desirable approach path of aircraft in landing phase will be studied in the sense of safety. The study was motivated by those successively happened accidents in Japan.

Many studies related to the safety of aircraft in landing phase have been done. One of the important directions of studies in theoretical treatment is the discussions based on the stability theory [*1–5*]. But the analyses of the low speed flight problems such as back side phenomenon of SST, STOL etc. by the stability theory do not include the discussions about the transient behaviours of the aircraft like flare.

Another distinct direction of studies is the application of optimal control theory, which is splitted into two phases. One is based on deterministic treatment and the other is on stochastic treatment. The application of well known regulator problem [*6*] to the automatic flight control system is considered to be the important former fruit in the sense of safety, because the stability around given nominal path

guarantees the safety itself [7]. Lately, it was shown that the regulator problem was applicable to nonlinear systems [8] and, also, the weighting matrices appearing in the quadratic performance index of the regulator problem were reasonably determined in engineering sense [9–10]. So it may be considered that the regulator problems are refined and are in practical use now [11]. However, these studies or theories about regulator problem can not teach us the method of determination of the nominal landing speed or path of aircraft.

One of the significant study in deterministic sense was performed by Komoda [12–13]. He deals with the controllable regions of engine failured helicopter and investigates the control procedures corresponding to the boundary of that regions. It seems to be remarkable in the sense of safety to use the concept of controllability, but such analytical study is not easy but needs deep insight about the objective dynamics and understandings of mathematical theory of optimal control.

The stochastic optimization technique is, on the other hand, important for Fujii and Shen proposed a paper [14] including pilot lag in control and errors in observation and investigated the minimum deviation from the objective state. But likely to stability theory, the unsteady flare maneuver is not included in that paper. Any way, as above mentioned, the flight path in approach has not been physically clarified or theoretically determined in relation to safety of the aircraft operation.

Present study is one of the trials to determine the approach path of the aircraft by considering the human safety and comfortability. The determination is performed by adding statistical considerations to the controllable height regions obtained for spot landings by numerical optimizations. This paper consists of three main subjects: investigations on the easier numerical method of obtaining the controllable region, the numerical expression of the controllable region of conventional aircraft in spot landings and the desirable approach speeds and paths in view of statistically safe landing.

It must be pointed out that, in this paper, errors of the values of aerodynamic derivatives of equation of motion of aircraft, errors of instruments, effects of gust on control surfaces of aircraft and control misses of pilot are not contained explicitly and assumed that the stability and maneuverability of aircraft may be left out of consideration.

2. Controllable and Reachable Regions

Mathematically speaking, the possibility of comfortable landing of an aircraft at a specified flight time T depends on whether the aircraft is always inside a T-controllable region or not, which is a set of initial state being controllable to a specified final state in time T under all constraints posed on state and control variables. Since one of the purposes of this paper is to investigate the T-controllable regions of aircraft in the landing phase, knowledge about the nature or equation of T-controllable region is necessary. Now a T-reachable region can, by similar way to T-controllable region, be defined as a set of final state to which a specified initial state is reachable in time T under all constraints. In this section,

the equation of T-controllable and reachable regions will simply be derived from the geometrical stand point, and the nature or mutual relations between them will be mentioned.

2–1 T-Controllable and T-Reachable Regions

Equations of the boundary of T-controllable and reachable regions were already introduced by Snow [*15*], but in the process of reduction of the equations he used some skillful but complicate techniques in treatment of control variables. Here, according to clarify the geometrical meaning, the conditional differential equations that may be called quasi Hamilton-Jacobi-Bellman equation (H-J-B equation) will be introduced and the mutual relation between T-controllable and reachable regions will be discussed.

(T-Controllable Region)

Let us consider the boundary of T-controllable region for a final manifold $M(x, t_f)=0$.

$$C(x, T)=0. \tag{2–1}$$

Then the boundary of $T+dT$-controllable region related to above equation as for the same manifold can be expressed as

$$C(x-dx, T+dT)=0 \tag{2–2}$$

where $-dx$ is an increment vector being reachable to a point on the $C(x,T)=0$ in time dT. Here, a gradient of C, C_x, is a vector defined to take minus direction of $C=0$ (Fig. 2–1). The condition that $C(x-dx, T+dT)$ attains its maximum value at the point $x-dx$ is needed because a point or points on C can coincide with the boundary of locally controllable region dC but the boundary of C can not intersect the boundary of dC. Of course, vector dx must satisfy the system equation of motion. Thus, the condition that must be satisfied in the controllable region are rearranged as follows:

$$\text{max. } C(x-dx, T+dT)=0 \tag{2–3}$$

$$C(x, T)=0 \tag{2–4}$$

$$\dot{x}=f(x, u) \tag{2–5}$$

Eqs. 2–3~2–5 reduce to limiting form of

$$\text{max. } (-C_x f+C_t)=0 \tag{2–6}$$

where

$$C_x=\left|\frac{\partial C}{\partial x_1}, \frac{\partial C}{dx_2}, \cdots, \frac{\partial C}{\partial x_n}\right|, \qquad C_t=\frac{\partial C}{\partial t}.$$

This is the desired relation describing the nature of T-controllable region with respect to $M(x, t_f)=0$.

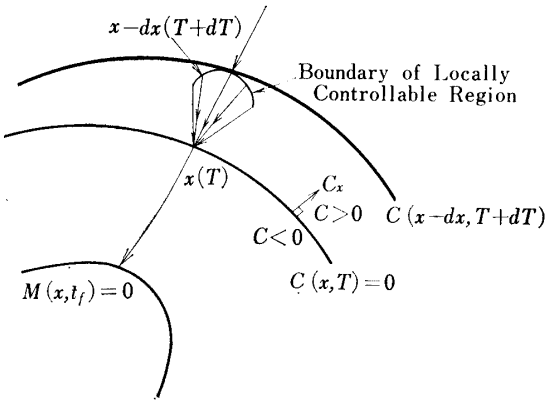

FIG. 2–1. Controllable region

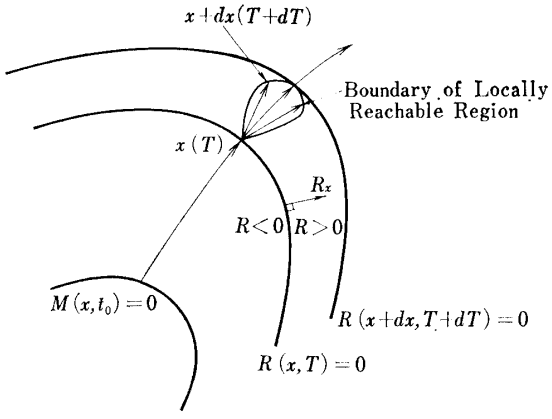

FIG. 2–2. Reachable region

(T-Reachable Region)

Similarly, two reachadle regions governed by $R(x, T)=0$ and $R(x+dx, T+dT)=0$ can be considered. A gradient of R, R_x, is defined to be vectored to the plus direction of $R=0$ (Fig. 2–2). Considering the nature of the boundary of locally reachable region dR, we can obtain the following relations:

$$\max.\ R(x+dX, T+dT)=0 \tag{2–7}$$

$$R(x, T)=0 \tag{2–8}$$

$$\dot{x}=f(x, u) \tag{2–9}$$

These are reduced to next equation by taking limiting process.

$$\max.\ (R_x f+R_t)=0 \tag{2–10}$$

where

$$R_x=\left|\frac{\partial R}{\partial x_1}, \frac{\partial R}{\partial x_2}, \cdots, \frac{\partial R}{\partial x_x}\right|, \qquad R_t=\frac{\partial R}{\partial t}.$$

This is the equation of the boundary of the T-reachable region with respect to an initial manifold $M(x, t_0)=0$.

If we consider a supposed calculation process of obtaining the coundary of T-controllable region in reversed time, then the movement of the objective system is reversed as if the system is started from the manifold $M(x, t_f)=0$, and the H-J-B equation to which the boundary of controllable region obeys is turned to

$$\max.\ (C_x f+C_t)=0. \tag{2–11}$$

This equation coincides with Eq. 2–10 which expresses the boundary of T-reachable region. From this fact, it is conludingly to say that the reachable region obtained by using the reverse time and the initial condition of $M(x,t_0)=0$, is nothing but the controllable region with respect to the initial condition of $M(x,t_0)=0$ [*15*].

(Nature of the Reachable Region)

Following characteristics of the reachable region are well known [*16*]:

1. If a system is linear and the set of control variable is bounded and convex, then the set of reachable region is also bounded and convex.
2. If a system is linear and the set of control variable is bounded and closed, then the maximum principle [*22*] gives the necessary and sufficient condition for the surface of the reachable set.

Unfortunately, in the current state, we can scarcely know about the mathematical natures of the reachable or controllable regions if a state variable constraint is added to a dynamic system such as an aircraft in airborne. On the other hand, it is exceedingly difficult to solve Eq. 2–3 or 2–7 directly in due consideration of computing time or high core memories of the computer [*17–19*]. The development of new numerical approach to the controllable or reachable regions of such dynamic system seems to be still valuable.

3. Two Phases Optimization Method

In this section, a numerical method of obtaining the reachable points is discussed for a system with first-order state-inequalities in the sense of Bryson [*24*]. Since the present method is based on linear programming and, as will be described later, this method consists of two step optimizing procedures, we want to call it TPO method which is a short designation for Two Phases Optimization method.

First step in TPO method is to constitute a locally optimal trajectory which is optimal for any impulsive variational controls. Second step is to optimizing switching points of the locally optimal trajectory. At a grance, the first step is considered to be unnecessary but as will be pointed out in later this process attains the important role for the optimizations because it economizes the large amount of computing time. Practically, time must be quantized into discrete increments and the calculation should begin with large time increments and smaller time increments should be taken by a degree as the growth of iteration number.

The TPO method has a clear limit that it can be applied only to the systems having linear control input. That is to say, this method utilizes the character of bang-bang control law which appears inherently in optimization of linear control systems [*22*].

3–1 Control Constraints

3–1–1 Formulation of the Problem

For the sake of simplicity, let us treat a linear system first. Here, the problem is to find a control that transfers the state from x_0 to some desired terminal state

$$Dx(t_f)+C=0 \tag{3–1}$$

so as to minimize the performance index of the form

$$x^0(t_f)=c'x(t_f), \tag{3–2}$$

under the restriction of a given linear system

$$\dot{x} = Ax + Bu \tag{3-3}$$

where

$$u \in \mathcal{U}(t), t_f : \text{fixed}.$$

3–1–2 Two Phases Optimization Method

The procedure of the TPO method is divided into the following three steps:

Step 1; Construction of Reference Trajectory

Since the TPO method is direct method, a reference trajectory which is an arbitrary initial path satisfying all constraints is required to begin with the calculation. This trajectory can easily be constructed by using a method which is introduced by taking a transformation from Euclid space to Hilbert space (Appendix A). In this paper, the method of obtaining the reference trajectory is to be called Sinnott's method naming after the reporter [*23*].

Step 2; Construction of Locally Optimal Trajectory in Narrow Sense

Hereinafter, the phrase "locally optimal in narrow sense" is used when the trajectory is optimal for any impulsive variational controls. To find a locally optimal trajectory, we consider first a variational control in a time interval which is quantized into some equi-length increments. The number of increments should be selected so as the variational controls in those increments can affect both of final state and performance index, and smaller number is prefered to simplify the discussion and to save the complexity of the computer program. In this time interval whose position is arbitrary at this time, the optimal variational or impulsive controls are determined so as to make the increment of performance index minimum satisfying the final condition. Then the time interval should be shifted to time increasing direction by just one increment and the procedure should be taken again. This process should be repeatedly executed. If the process reaches the specified final time, the procedure should be returned to initial time and repeated again. The locally optimal trajectory in narrow sense is expected as the converged result of these calculations. As a matter of course, the obtained control has a bang-bang characteristics.

Step 3; Optimization of Switching Points

In this step, some variations to the switching points are provided to minimize the accompanied increment of performance index or to improve the locally optimal trajectory which is gotten as the result of Step 2. Iteration is necessary because the variation of the switching points is restricted to one block of time increment in one calculation and this procedure is based on the linear programming. The converged results satisfy the final conditions and, in fact, have the bang-bang control characteristics which are derived by the maximum principle. Apparently, the above calculation procedure results that the converged trajectory has better performance index than those of neighbourhoods. If the above described iteration

is converged, then the corresponding trajectory satisfies the necessary condition for optimality of the problem formulated in 3–1–1.

3–1–3 Locally Optimal Trajectory in Narrow Sense

In this subsection, the locally optimal trajectory in narrow sense is shown to be able to construct by using the linear programming.

The terminal state of the system described by Eq. 3–3 at the final time t_f is

$$x(t_f)=\phi(t_f, t_0)\Big[X_0+\int_{t_0}^{t_{p1}}\phi^{-1}(t, t_0)Bu_N dt + \int_{t_{p1}}^{t_q}\phi^{-1}(t, t_0)Bu_N dt+\int_{t_q}^{t_f}\phi^{-1}(t, t_0)Bu_N dt\Big] \tag{3–4}$$

where a transition matrix $\phi(t, t_0)$ satisfies

$$\dot{\phi}(t, t_0)=A\phi(t, t_0) \tag{3–5}$$

$$\phi(t_0, t_0)=I \tag{3–6}$$

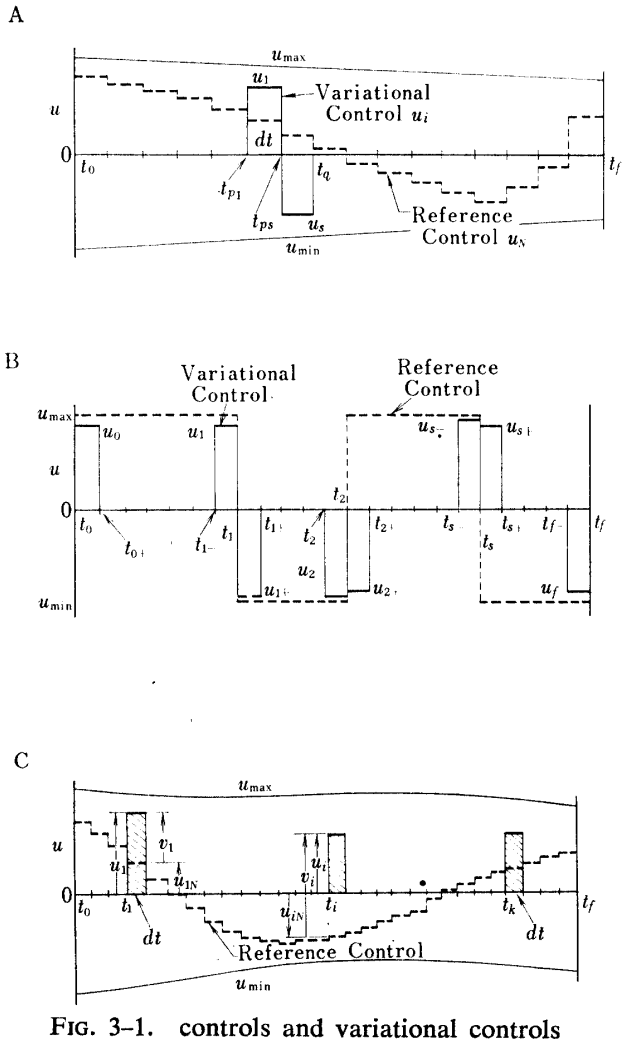

FIG. 3–1. controls and variational controls

and t_0 is an initial time, (t_{p1}, t_q) is an arbitrary time interval, and subscript N indicates the reference state (Fig. 3–1A). The candidate control $u(t)$ for optimality in the time interval (t_{p1}, t_q) moves the termimal state to

$$x(t_f)=\phi(t_f, t_0)\Big[x_0+\int_{t_0}^{t_{p1}}\phi^{-1}(t, t_0)Bu_N dt + \int_{t_{p1}}^{t_q}\phi^{-1}(t, t_0)Budt+\int_{t_q}^{t_f}\phi^{-1}(t, t_0)Bu_N dt\Big]. \tag{3–7}$$

Accordingly, the variation vector of the terminal state by the candidate control becomes

$$\begin{aligned} dx(t_f)&=x(t_f)-x_N(t_f)\\ &=\phi(t_f, t_0)\int_{t_{p1}}^{t_q}\phi^{-1}(t, t_0)Budt-\phi(t_f, t_0)\int_{t_{p1}}^{t_q}\phi^{-1}(t, t_0)Bu_N dt. \end{aligned} \tag{3–8}$$

Now, let us divide the time interval (t_{p1}, t_q) into s equi-length increments. Then the Eq. (3–8) is rewritten as

$$dx(t_f)=\phi(t_f, t_0)\Big[\sum_{i=1}^{s}\phi^{-1}(t_{pi+1}, t_0)Bu_i dt-\sum_{i+1}^{s}\phi^{-1}(t_{pi+1}, t_0)Bu_{iN}dt\Big]. \tag{3–9}$$

On the other hand, from the relation of

$$dx_{pi}=[Ax(t_{pi})+Bu_{iN}]dt, \tag{3–10}$$

we get

$$Bu_{iN}dt=dx_{pi}-Ax(t_{pi})dt. \tag{3–11}$$

From Eqs. 3–9 and 3–11, we obtain

$$dx(t_f)=\phi(t_f, t_0)\Big[\sum_{i=1}^{s}\phi^{-1}(t_{pi+1}, t_0)Bu_i dt - \sum_{i=1}^{s}\phi^{-1}(t_{pi+1}, t_0)[dx_{pi}+Ax(t_{pi})dt]\Big]. \tag{3–12}$$

Now, since the transition matrix ϕ has the characteristics of

$$\phi(t_f, t_0)\phi^{-1}(t_{pi+1}, t_0)=\phi(t_f, t_0)\phi(t_0, t_{pi+1})=\phi(t_f, t_{pi+1}), \tag{3–13}$$

ϕ^{-1} in Eq. (3–12) can be eliminated and the following new relation can be obtained:

$$dx(t_f)=\sum_{i=1}^{s}\phi(t_f, t_{pi+1})[Bu_i dt-(dx_{pi}-Ax(t_{pi}))dt]. \tag{3–14}$$

Applying this relation into Eq. (3–1), the variation of the performance index by the candidate control u_i is obtained as

$$dx^0(t_f)=c'dx(t_f)=c'\Big[\sum_{i=1}^{s}\phi(t_f, t_{pi+1})\{Bu_i dt-(dx_{pi}-Ax(t_{pi})dt)\}\Big]. \tag{3–15}$$

Using a transformation of

$$\bar{u}_i \triangleq u_{\max} - u_i, \tag{3-16}$$

the problem of obtaining the optimal impulsive variational control can be re-arranged in summation form as follows:

Constraints

$$\bar{u}_i \geqq 0 \tag{3-17}$$

$$u_{\max} - u_{\min} - \bar{u}_i \geqq 0, \qquad i = 1 \sim s \tag{3-18}$$

$$D \sum_{i=1}^{s} \phi(t_f, t_{pi+1})[Bu_{\max} dt - (dx_{pi} - Ax(t_{pi})dt)] - D \sum_{i=1}^{s} \phi(t_f, t_{pi+1}) B\bar{u}_i dt = 0 \tag{3-19}$$

Performance Index

$$\text{min. } dx^0 = -c' \sum_{i=1}^{s} \phi(t_f, {}_{pi+1}) B\bar{u}_i dt \tag{3-20}$$

where $\bar{u}_i$ are the unknown controls.

This is a linear programming problem itself [27]. Solving this problem iteratively until it converges according to the procedure cited in 3–1–2, we can obtain the locally optimal trajectory in narrow sense.

3–1–4 Optimization of Switching Points

Here, both of the controls at discrete time increment of terminal point and at opposite sides of each switching point are selected as the variational controls (cf. 26). The final state of the reference trajectory is, as in 3–1–3, given by

$$\begin{aligned} x_N(t_f) = \phi(t_f, t_0) \Bigg[& x_0 + \int_{t_{0+}}^{t_{1-}} \phi^{-1}(t, t_0) Bu_N dt + \sum_{i=1}^{s-1} \int_{t_{i+}}^{t_{(i+1)-}} \phi^{-1}(t, t_0) Bu_N dt \\ & + \int_{t_{s+}}^{t_{f-}} \phi^{-1}(t, t_0) Bu_N dt + \phi^{-1}(t_{0+}, t_0)(dx_{p0} - Ax(t_0)dt) \\ & + \phi^{-1}(t_f, t_0)(dx_{pt_f} - Ax(t_{f-})dt) + \sum_{i=1}^{s} \{\phi^{-1}(t_i, t_0)(dx_{pi} \\ & - Ax(t_{i-})dt) + \phi^{-1}(t_{i+}, t_0)[dx_{pi+} - Ax(t_i)dt]\} \Bigg], \end{aligned} \tag{3-21}$$

where t_0, t_f, t_i $(i = 1 \sim s)$ are switching times, $u_0, u_{1-}, u_{1+}, \cdots, u_{s-}, u_{s+}, u_{tf}$ are the controls at the switching points, $t_{i\mp}$ are time just before or after the switching point $t = t_i$ and $dx_{pi,pi+}$ is a movement of x_N in a time difference before or after the switch t_i. The final point of the trajectory corrected by new variational controls is obtained as same way

$$\begin{aligned} x(t_f) = \phi(t_f, t_0) \Bigg[& x_0 + \int_{t_{0+}}^{t_{1-}} \phi^{-1}(t, t_0) Bu_N dt + \sum_{i=1}^{s-1} \int_{t_{i+}}^{t_{(i+1)-}} \phi^{-1}(t, t_0) Bu_N dt \\ & + \int_{t_{s+}}^{t_{f-}} \phi^{-1}(t, t_0) Bu_N dt + \phi^{-1}(t_{0+}, t_0) Bu_0 dt + \phi^{-1}(t_f, t_0) Bu_{tf} dt \\ & + \sum_{i=1}^{s} \{\phi^{-1}(t_i, t_0) B_{i-} dt + \phi^{-1}(t_{i+}, t_0) Bu_{i+} dt\} \Bigg]. \end{aligned} \tag{3-23}$$

From Eqs. 3–21 and 3–22, we can obtain the variation of the final state of the trajectory by applying new variational controls.

$$\begin{aligned} dx(t_f) = x(t_f) - x_N(t_f) = -\phi(t_f, t_0)\Big[& \phi^{-1}(t_{0+}, t_0)[dx_{p0} - Ax(t_0)dx] \\ & + \phi^{-1}(t_f, t_0)(dx_{pt_f} - Ax(t_{f-})dt) \\ & + \sum_{i=1}^{s} \{\phi^{-1}(t_i, t_0)(dx_{pi} - Ax(t_{i-})dt) + \phi^{-1}(t_{i+}t_0)(dx_{pi+} - Ax(t_i)dt)\}\Big] \\ & + \phi(t_f, t_0)\Big[\phi^{-1}(t_{0+}, t_0)Bu_0 dt + \phi^{-1}(t_f, t_0)Bu_{tf}dt \\ & + \sum_{i=1}^{s} \{\phi^{-1}(t_i, t_0)Bu_{i-} \cdot dt + \phi^{-1}(t_{i+}, t_0)Bu_{i+} \cdot dt\}\Big]. \end{aligned} \tag{3–23}$$

Using the characteristics of transition matrix, we can eliminate the inverse matrices and obtain the next relation:

$$\begin{aligned} dx(t_f) = -\Big[& \phi(t_f, t_{0+})(dx_{p0} - Ax(t_0)dt) + \phi(t_f, t_f)(dx_{pt_f} - Ax(t_{f-})dt) \\ & + \sum_{i=1}^{s} \{\phi(t_f, t_i)(dx_{pi} - Ax(t_{i-})dt) + \phi(t_f, t_{i+1})(dx_{pi+} - Ax(t_i)dt)\}\Big] \\ & + \Big[\phi(t_f, t_{0+})Bu_0 dt + \phi(t_f, t_f)Bu_{tf})Bu_{tf}dt \\ & + \sum_{i=1}^{s} \{\phi(t_f, t_i)Bu_{i-}dt + \phi(t_f, t_{i+})Bu_{i+}dt\}\Big]. \end{aligned} \tag{3–24}$$

Now, the problem is to minimize the increment of performance index under the restriction of $Dx(t_f)+C=0$ and $u \in \mathcal{U}$. Same transformations as the preceeding section would be used, which are written as

$$\bar{u}_{i\pm} \triangleq u_{\max} - u_{i\pm}. \tag{3–25}$$

Thus, the standard linear programming problem for the optimization of switching points is obtained as follows:

Linear Programming Problem

Constraints

$$\bar{u}_0, \bar{u}_{tf}, \bar{u}_{i\pm} \geqq 0 \qquad (i = 1 \sim s) \tag{3–26}$$

$$u_{\max} - u_{\min} - \bar{u}_0 \geqq 0 \tag{3–27}$$

$$u_{\max} - u_{\min} - \bar{u}_{tf} \geqq 0 \tag{3–28}$$

$$u_{\max} - u_{\min} - \bar{u}_{i-} \geqq 0 \qquad (i = 1 \sim s) \tag{3–29}$$

$$u_{\max} - u_{\min} - \bar{u}_{i+} \geqq 0 \qquad (i = 1 \sim s) \tag{3–30}$$

$$\begin{aligned} D\Big[& -\phi(t_f, t_{0+})(dx_{p0} - Ax(t_0)dt) + \phi(t_f, t_f)[dx_{pt_f} - Ax(t_{f-})dt] \\ & + \sum_{i=1}^{s} \{\phi(t_f, t_i)(dx_{pi} - Ax(t_{i-})dt) + \phi(t_f, t_{i+})(dx_{pi+} - Ax(t_{i+})dt)\}\Big] \end{aligned}$$

$$-D\Big[\phi(t_f, t_{0+})B\bar{u}_0 dt+\phi(t_f, t_f)B\bar{u}_{tf}dt$$
$$+\sum_{i=1}^{s}\{\phi(t_f, t_i)B\bar{u}_{i-}dt+\phi(t_f, t_{i+})B\bar{u}_{i+}dt\}\Big]=0 \tag{3-31}$$

Performance Index

$$\text{min. } dx^0=-c'\Big[\phi(t_f, t_{0+})B\bar{u}_0 dt+\phi(t_f, t_f)B\bar{u}_{tf}dt$$
$$+\sum_{i=1}^{s}\{\phi(t_f, t_i)B\bar{u}_{i-}dt+\phi(t_f, t_{i+})B\bar{u}_{i+}dt\}\Big] \tag{3-32}$$

Solving this problem, we can improve the switching points. Hence the switching points are movable only one time increment in each calculation, the iteration procedure is necessary. When the variation of performance index is converged, the corresponding trajectory may be regarded as locally optimal in an ordinary sense.

When the system contains high dimensional control variables, additional iterations should be taken reciplocally for each element of control vector in order to save the computing time. Namely, only one element of the control vector should be taken as a variational control in a series of optimizing calculations and this optimization should be continuously taken by turns for each control element until the convergence of performance index for all control elements is assured. These modifications saves the increase of complexity of computer programs for the higher control dimensional problems because the program is obtained simply by adding a little change to that of scalar control problem.

3–1–5 Extension to Nonlinear Problem

The TPO method can be applied to nonlinear problem if the control variables are still linear in the system equation.

In this case, the system equation, instead of Eq. 3–3, is expressed as

$$\dot{x}=f(x)+Bu, \tag{3-33}$$

and the other conditions are same as those stated in 3–1–1. The variation of the final state from the reference state is

$$dx(t_f)=\sum_{i=1}^{k}\phi(t_f, t_i+dt)Bv_i dt \tag{3-34}$$

$$v_i=u_i-u_{Ni} \qquad (i=1\sim k) \tag{3-35}$$

$$\dot{\phi}(t, t_0)=f_x\phi(t, t_0) \tag{3-36}$$

$$\phi(t_0, t_0)=I, \tag{3-37}$$

for k variational controls. Using Eqs. 3–2, 3–3 and 3–4, the optimal correction of the control variables can be stated likely to the case of linear systems as follows:

Constraints

$$D\sum_{i=1}^{k}\phi(t_f, t_i+dt)Bv_i dt=0 \tag{3-38}$$

$$v_i+u_{Ni}\geqq u_{\min} \qquad (i=1\sim k) \tag{3-39}$$

$$v_i+u_{Ni}\leqq u_{\max} \qquad (i=1\sim k) \tag{3-40}$$

Performance Index

$$\min dx^0=c'\sum_{i=1}^{k}\phi(t_f, t_i+dt)Bv_i dt \tag{3-41}$$

What is different from the linear case is the dependence of the transition matrix $\phi(t, t_0)$ on reference controls and trajectory which vary with each iteration (Eq. 3–36). This difference means the necessity of large increase of computation time in nonlinear case.

3–2 First-Order State-Inequality-Constraint

3–2–1 Formulation of the Problem

As for the oscillatory systems in state constrained space, we can not know in advance that how many times the optimal solution rides on the boundary of the constraint. It is difficult to solve these problems by indirect method due to the sensitivity and complexity of boundary value problem [*20–25*]. These problems can be solved by modifying the TPO method, if the optimal trajectory on the constraint boundary can be determined analytically.

We consider the minimization of the performance index of Eq. 3–2 subject to Eqs. 3–1 and 3–3 under the additional state-inequality-constraint

$$g=Px+q\geqq 0 \tag{3-42}$$

$$\frac{\partial}{\partial u}(\dot{g})\neq 0 \tag{3-43}$$

3–2–2 TPO Method with First-Order State-Inequality-Constraint

Calculation procedure of the TPO method for state constrained problem is shown below.

Step 1: Construction of Reference Trajectory

Using Sinnott's method, we can construct from an arbitrary initial trajectory a proper reference trajectory which satisfies all necessary constraints. If we do not require the optimality to the reference trajectory, it is not so difficult to satisfy the state constraints.

Step 2: Construction of Locally Optimal Trajectory in Narrow Sense that Satisfies the State-Inequality-Constraints

The process of the construction of solution in this case is same as that of the state free case fundamentarily. A new restriction that controls must satisfy $g\geqq 0$ at the beginning of the continued time interval of $g<0$ should be added. If the controls satisfying the above new restriction do not exist, a trajectory which is

optimal on the constraint boundary should be constructed to move on the boundary from the time of $g \leqq 0$ to the time of $g > 0$. After the exit point, the same procedure as state free case should be taken. The method of iteration itself is also same as the state free case. The impulsive variational control is taken iteratively to the time increasing direction in order. Doing above procedure, we can get a solution for the trajectory in converged form satisfying the state constraints and the locally optimality in narrow sense. Then we can go to the next step.

Step 3: Optimization of Switching Points

Here, only switching and exit points should be taken as variational control variables. In this step, proper number of iteration for the minimization of performance index must be taken to improve the trajectory obtained in Step 2 without thinking of state constraint.

Step 4: Iteration of Step 2 and Step 3

The procedure of Step 2 and Step 3 must be taken repeatedly. If the performance index in Step 2 shows the oscillatory nature, reduce the number of iteration in Step 3. If this nature doesn't diminish even in one iteration number in Step 3, the smaller value of performance index should be regarded as the ptimal value.

3–2–3 Locally Optimal Trajectory in Narrow Sense

The constraints that must be added in this case to the formulation in section 3–1–3 are shown below.

On the state constraint boundary, next relations must be satisfied:

$$g = Px + q \geqq 0 \tag{3-44}$$

$$\dot{g} = P\dot{x} \geqq 0 \tag{3-45}$$

Substituting the following relations:

$$dx = (Ax + Bu_i)dt \tag{3-46}$$

$$\bar{u}_i = u_{\max} - u_i \tag{3-47}$$

into Eq. 3–45, we can obtain

$$P(Ax + Bu_{\max} - B\bar{u}_i)dt \geqq 0. \tag{3-48}$$

This is the new restriction that should be imposed at the time of $g \leqq 0$.

3–2–4 Optimization of Switching Points

The method of variation of switching points should be treated entirely same as the state free case. Using Eqs. 3–26 and 3–32, the switching points and entry or exit points can be revised. Additional variational controls are required at the exit point to determine the way of movings of the trajectory at that point; keeping along or departing from the constraint boundary.

3–3 Numerical Examples of TPO Method

3–3–1 Control Constraints

Example 1. Oscillatory System

System Equation

$$\dot{x}_1 = x_2 + u_1 \tag{3-49}$$

$$\dot{x}_2 = -x_1 - x_2 + u_2 \tag{3-50}$$

Constraints

$$|u_1| \leqq 0.85, \quad |u_2| \leqq 0.85, \quad x_1(0) = 1.0, \quad x_2(0) = 1.0$$
$$x_1(t_f) + x_2(t_f) = 0.15 \qquad t_f = 8.192$$

Performance Index

$$\text{min. } x^0(t_f) = x_1(t_f) \tag{3-51}$$

Since the Hamiltonian and adjoint equations are written as

$$\mathscr{H} = -x_2 + x_1\phi_1 - (x_1 + x_2)\phi_2 + (-1 + \phi_1)u_1 + \phi_2 u_2 \tag{3-52}$$

$$\dot{\phi}_1 = \phi_2 \tag{3-53}$$

$$\dot{\phi} = 1 - \phi_1 + \phi_2, \tag{3-54}$$

the optimal control law derived from the maximum principle is described as below:

$$u_{1opt} = \text{sign } (-1 + \phi_1) \tag{3-55}$$

$$u_{2opt} = \sin \phi_2 \tag{3-36}$$

These relations show that the optimal controls are bang-bang, and that the switching interval of the optimal controls is half the natural frequency of the system.

The numerical results gotten by giving the variation controls u_1 and u_2 reciprocally are shown in Fig. 3–2. We can see that the numerical result satisfies the optimal characteristics obtained by the maximum principle.

3–3–2 State Constrained Case

The flow chart of the TPO method in the state constrained case is shown in Fig. 3–3. There, the procedure which corresponds to state free TPO method is simply expressed as

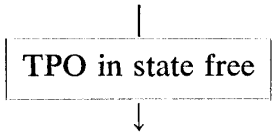

Example 2. Oscillatory System Having Velocity Limit

System Equation

$$\dot{x}_1 = x_2 \tag{3-57}$$

$$\dot{x}_2 = -x_1 - x_2 + u \tag{3-58}$$

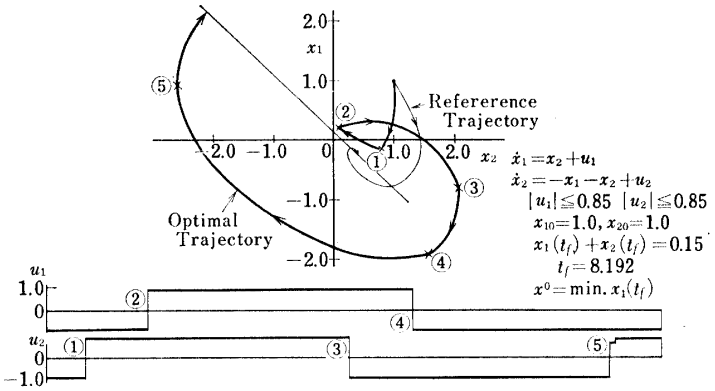

FIG. 3–2. Numerical example of TPO method: converged trajectory and controls

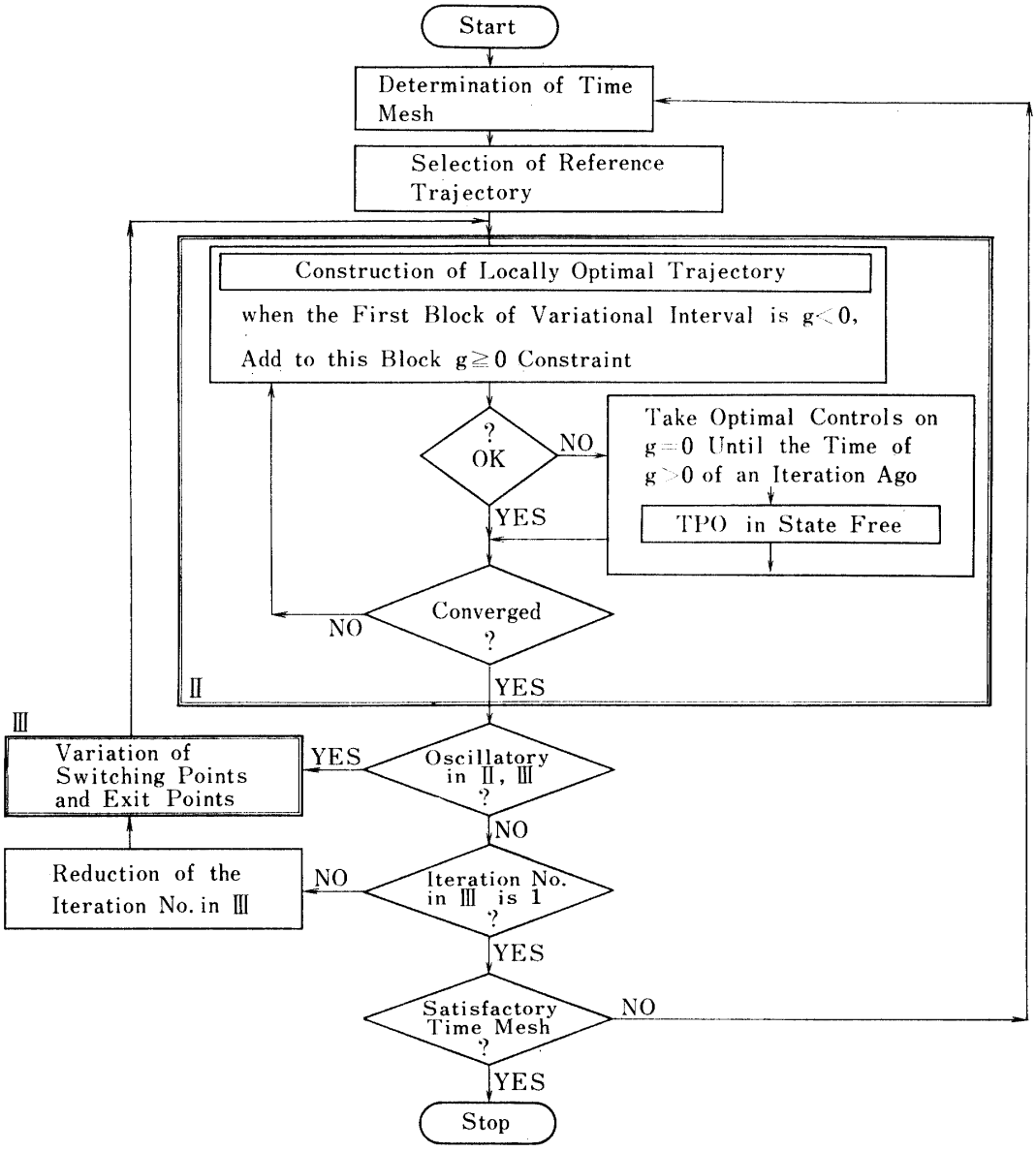

FIG. 3–3. Flow chart of TPO method in state constrained case

Constraints

$$|u| \leqq 1.0, \quad x_1(0)=1.0, \quad x_2(0)=1.0$$
$$x_2(t_f)=0.1, \qquad t_f=8.192$$
$$g=x_2+0.8 \geqq 0$$
$$\left(\frac{\partial}{\partial u}\dot{g}=1 \neq 0\right) \tag{3-59}$$

Performance Index

$$\text{min. } x^0(t_f)=x_1(t_f) \tag{3-60}$$

The maximum principle says that the optimal solution in the state free region has bang-bang characteristics, but it doesn't teach us anything about the entry and exit points. Calculated results by the TPO method are shown in Figs. 3–4~3–6. In this calculation, three kinds of discrete time increment are taken: total time is constructed by 32, 128 and 512 meshes. Illustrated in Fig. 3–4 are aspects of

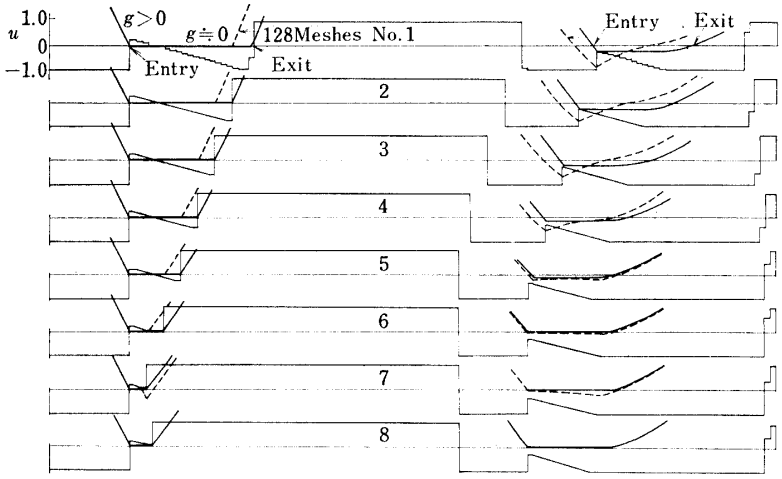

FIG. 3–4. Movements of entry and exit points in Example 2

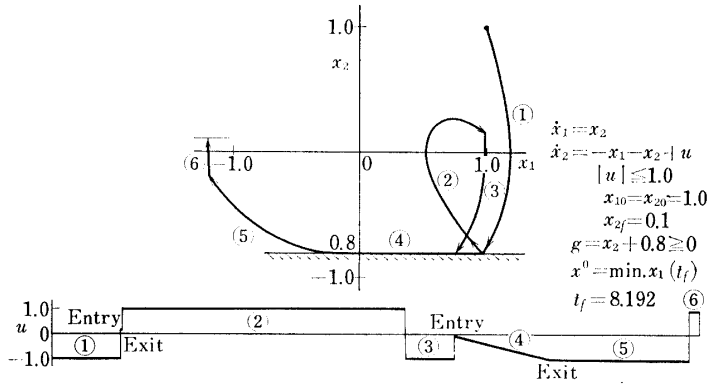

FIG. 3–5. Numerical example of TPO method in state constrained case: converged trajectory and control

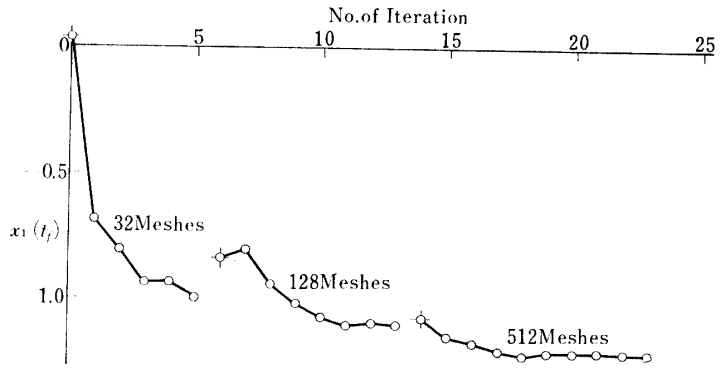

FIG. 3–6. Aspect of convergence of TPO methop in Example 2

movements of switching, entry and exit points in 128 time meshes with the increase of iteration number. Solid line shows the improved results at Step 2 and broken line shows the results of Step 3 in the sense of 3–2–2. In Fig. 3–5, the converged result at 512 time meshes is shown on the phase plane. It is interesting to note that the first entering to the state constraint boundary is reflected immediately, and the final exit from the boundary is smooth. The aspect of convergences is illustrated in Fig. 3–6 for each time meshes.

3–4 Characteristics of the TPO Method

Merits of the TPO method may be described as follows:

1. The procedure can easily be understood in theoretical view point.
2. The problem of obtaining the reachable points with first-order state-inequality-constraint can be solved directly when the optimal trajectory on the constrained boundary can be determined analytically.
3. Arbitrary time meshes may be selected according to the user's purposes as far as the high speed memory of the computer is not violated. When the purpose is to obtain the qualitative aspects of optimal trajectories in short computing time, a coarse time mesh should be selected, on the contrary, when a correct optimal solution is desired, fine time mesh should be selected.

Demerits of the TPO method can be listed as follows:

1. The method is only applicable to the problems of obtaining the reachable points of linear control systems. In other words, the optimal solution of the problem must be bang-bang.
2. Computer program must be complex for the problem with state inequality constraint.
3. The optimality in global sense can not be discussed with this method.

As we have seen, the TPO method has several features. When we are interested in the controllable regions of aircraft in spot landing, the angle of attack constraint stands as an unovercoming barriers in our way of investigation because of its first order characteristics in sense of Bryson. This is the motivation of development of the TPO method. In this paper, concrete calculations about aircraft landings are executed by the TPO method.

4. Numerical Procedures for Obtaining the Controllable Height Regions of Aircraft in Landing

Before the discussion of the effects of approach velocity and path angle on safe landings, it is necessary to obtain the controllable height regions of aircraft in landing. Although the controllable regions for all variables in state space are desirable for the present discussion, it is unrealizable to obtain such regions specifically for high dimensional problems with state constraints as those of aircraft landing.

In this paper, we assume that the aircraft is in steady state at initial time. The method of obtaining the controllable height will be discussed under this condition. We use velocity U and approach path angle γ as the parameters which specify the steady state of the aircraft.

4–1 Equation of Motion of Aircraft

The longitudinal linearized equation of motion of aircraft which contains the moment equation [*28, 33*] will be treated for simplicity, for we want to know the control law of aircraft in short period of time. We neglect the change of air density with respect to height and the ground effect to landing performance of the aircraft.

A differential equation of motion in vectorial form is given by

$$\dot{x}=Ax+Bu. \tag{4–1}$$

If we consider the short period mode only, each element of state vector and coefficient matrices are given by

$$x'=|x_1, x_2, x_3, x_4|$$

$$x_1=\theta, x_2=\theta, x_3=\dot{h}, x_4=h$$

$$A=\begin{vmatrix} a_{11}a_{12}\cdots a^{14} \\ a_{21}a_{22}\cdots a_{24} \\ \cdots\cdots \\ a_{41}a_{42}\cdots a_{44} \end{vmatrix}, \qquad B=\begin{vmatrix} b_{11} \\ b^{12} \\ \vdots \\ b_{41} \end{vmatrix},$$

where θ and h means nondimensional incremental pitch angle and height, u means incremental elevator angle and $(\cdot)$ means the differentiation with respect to nondimensional time $\hat{t}$.

4–1–2 Formulation of the Problem

The problem is to obtain the upper and lower limits of the controllable height of aircraft that assures safe landings at a specified point on run-way, under the restriction of control quantity, angle of attack and presence of the ground. In this paper, the approach speed of aircraft is assumed to be maintained constant for simplicity and for the convenience of the discussions in section 5. Lateral motion is neglected here. Also, we require the aircraft must satisfy the next final condition for the rate of descent at touch down.

$$\boldsymbol{h}(t_f)=-0.3m/s \tag{4–2}$$

Pitch angle and pitch rate at touch down are to be investigated for each trajectory whether they are allowable values or not.

4–1–3 Aircraft Models

Hereinafter, a middle size transport aircraft with twin turbo-prop engines is designated as aircraft-1 which has following six flight phases:

1. Max. dynamic pressure flight
   (15,400 ft height, 295 kts speed)
2. Max. velocity flight
   (13,600 ft, 245 kts)
3. Cruising
   (20,000 ft, 180 kts)
4. Wave off
   (151 kts, gear up)
5. Approach-1
   (110 kts, gear down, 20 deg. flap down)
6. Approach-2
   (97 kts, gear down, 35 deg. flap down)

Since we pay attention to landing approach, the 4-th to 6-th phases are considered to be important. We choose 6-th phase mainly among them as our numerical example, and the other two phases are calculated only for the sake of comparison. Stability derivatives which are translated into coefficient form such as A or B are shown in Table 1. The stability derivatives of another middle size aircraft model designated as aircraft-2 are also shown in Table 2 for comparison.

4–2 Upper Boundary of Controllable Height Region

The fact that Eq. 4–1 doesn't contain the height term in right hand side indicates that corresponding trajectory keeps same forms irrespective of initial or final height if the same controls are taken. Thus, we can obtain a point of the initial upper boundary of controllable height region by changing the sign of performance index of the minimum height problems in order time for given steady state initial conditions and final descent rate. That is to say, the upper boundary of controllable height is given by adding the inverse sign of the final height to the reference path*. The final height is obtained by solving the following problem:

$$\dot{x}=Ax+Bu \tag{4–3}$$

$$x(t_0)=x_0 \tag{4–4}$$

$$x_3(t_f)=x_{3f} \tag{4–5}$$

$$\min.\ x^0=x_4(t_f) \tag{4–6}$$

* This method is applicable only when the ground does not exist on the way to the touch down point or when, as a results, the optimal path does not have the negative rate of descent. When the optimal path has the negative rate of descent, we must reformulate the problem as follows: The max. height is given as the solution of inverse time maximume height problems with $h \geqq 0$.

4–2–1 Constraint of Elevator Angle

It is sufficient in this case to add the next control constraints on the elevator angle to Eqs. 4–3~4–6 for obtaining the upper boundary of the controllable region.

$$u \leqq u_{\max} \tag{4–7}$$

$$u \geqq u_{\min} \tag{4–8}$$

Points on the boundary of controllable height region for the elevator angle constraints can easily be obtained by using the TPO method. The solution of the maximum initial height problem for the case of

$$u_{\max} = 0.195 \tag{4–9}$$

$$u_{\min} = -0.255, \tag{4–10}$$

with the initial condition of level flight and with the flight distance of 1/2 naut mile is shown in Fig. 4–1. This figure shows that the optimum controls for the maxi-

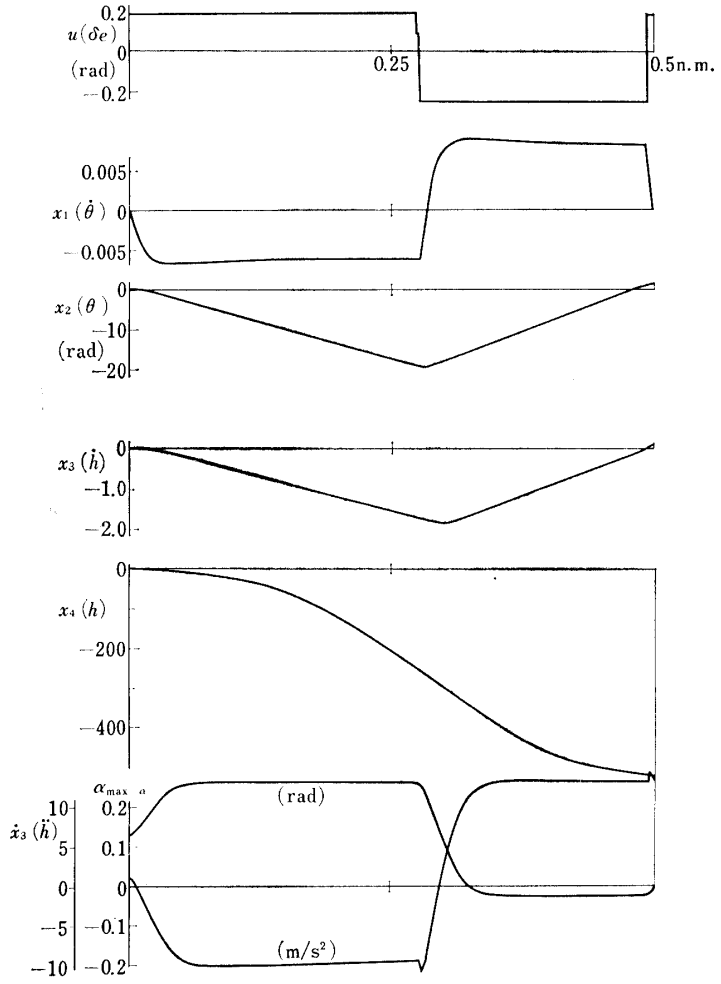

FIG. 4–1. Optimal control and trajectories for maximum initial height: aircraft–1, approach–2, U=49.9 m/s, $\gamma_0=\Theta_0=-2.5$ deg., $-0.255 \leqq \delta_e \leqq 0.195$

mum initial height are constructed by the steps of initial full nose down and second full nose up and final short time elevator full down maneuvers. The final maneuver indicates that the instantaneous lift of tail wing should be utilized in strictly speaking.

4–2–2 Attitude Constraint

Fig. 4–1 shows, however, the minimum pitching angle of the aircraft from the maximum height is excessive for the transportation of passengers, so we need to set the attitude angle constraint if a long time flight becomes an issue.

Attitude constraint is given by

$$\Theta \geqq \Theta_{\min}. \tag{4–11}$$

This is, by using the nondimensional pitch angle x_2, rewritten as follows:

$$x_2 \geqq x_{2\min}, \tag{4–12}$$

which is the second-order state-inequality-constraint. The TPO method can not be applied directly to the problem having second-order constraint. Although the well known method to attack these problems is to treat the entry and exit points indirectly by using the jump condition of the maximum principle, we would try to solve here by the direct method because of the some peculiar nature of the stated problem. Let us assume that an optimal path in case of attitude constraint is made of three segments: interior segment of a bounded space which moves to entry or from exit point named subarc 1 or 3 and segment on the constraint boundary named subarc 2.

Subarc 1. (Optimal Path Before Entering the Constraint Boundary)

The entering conditions that guarantee the movability of a point along the attitude constraint boundary are expressed by using 2-nd order characteristics of the constraint as

$$x_2 = x_{2\min} \tag{4–13}$$

$$\dot{x}_2 = 0. \tag{4–14}$$

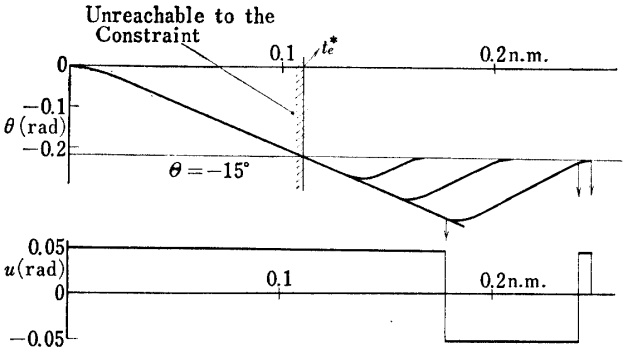

FIG. 4–2. Optimal trajectories which enter into attitude constraint smooth: min h, aircraft-1, approach–2, $\gamma_0=\Theta_0=-2.5$ deg.

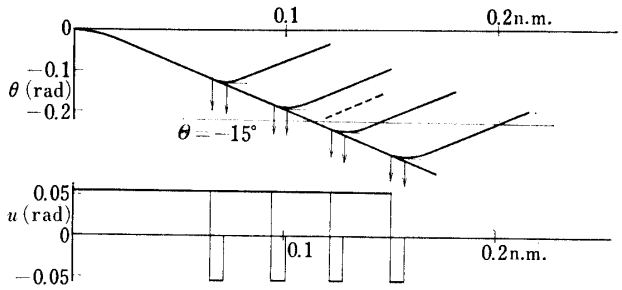

FIG. 4–3. Construction of optimal trajectory which enters into attitude constraint smooth and does not violate the constraint before the entry: min h, aircraft-1, approach-2, $\gamma_0=\Theta_0=-2..5$ deg.

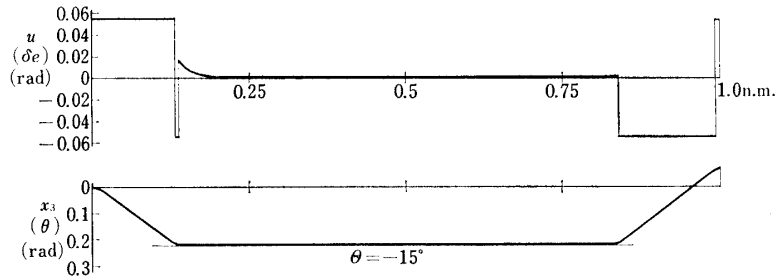

FIG. 4–4. Optimal control and trajectory which gives upper height gives upper height boundary in attitude constrained case: aircraft-1, approach-2, U=49.9 m/s, $\gamma_0=\Theta_0=-2.5$ deg., $|\delta_e|\leqq 0.055$

With the trial and error method, it is probably concluded in this case that only one optimal subarc which satisfies Eqs. 4–14 and 4–14 at the entry point exists (Figs. 4–2, 4–3). This is the aforementioned peculiar nature.

Subarc 2, 3. (On and From the Constraint Boundary)

The following relation is utilized to determine the controls to move along the constraint boundary:

$$\ddot{x}_2=a_{11}x_1+a_{12}x_2+a_{13}x_3+b_{11}u=0. \tag{4–15}$$

We can get the optimal subarcs by the TPO method as was described in section 3–2–2, because the remaining problem is only to determine the exit and switching points. Calculated results for the case of 1.0 naut mile distance, approach-2 phase and $\Theta\geqq -15°$ is shown in Fig. 4–4.

4–2–3 Angle of Attack Constraint

Wing angle of attack can be written as

$$\alpha=\alpha_0+{}'\alpha \tag{4–16}$$

where α_0 is the angle of attack in trimmed state and $'\alpha$ is variation from α_0. By using nondimensional rate of ascent h and variational pitch angle of aircraft θ, the non-dimensional rate of ascent is expressed as

$$\dot{h}=\theta-{}'\alpha \tag{4–17}$$

From these two equations, we have

$$\alpha=\alpha_0+\theta-\dot{h}. \tag{4-18}$$

This can be reduced to

$$\alpha=\alpha_0+x_2-x_3. \tag{4-19}$$

Therefore, we have next condition as the angle of attack constraint:

$$g_{(\alpha)}\triangleq -x_2+x_3+(\alpha_{\max}-\alpha_0)\geqq 0. \tag{4-20}$$

This is a first-order state-inequality-constraint because

$$\dot{g}_{(\alpha)}=-\dot{x}_2+\dot{x}_3=-x_1+(a_{31}x_1+a_{32}x_2+a_{33}x_3+b_{31}u) \tag{4-21}$$

$$\frac{\partial \dot{g}_{(\alpha)}}{\partial u}=b_{31}\neq 0. \tag{4-22}$$

Unfortunately, our TPO method is applicable to this problem in only partial case, for the control power of the aircraft is some times too small to move the aircraft at once along the constraint boundary. This aspect of affairs is easily understood by the next relation (Table 1):

TABLE 1. Coefficient Matrices of Fquation of Motion of Aircraft-1

1. Approach-2: flap down (35 deg.), U=49.9 m/sec

$$A=\begin{vmatrix} -0.001140 & -0.05602 & 0.001132 & 0.0 \\ 0.0 & 1.0 & 0.0 & 0.0 \\ 0.05162 & 0.07023 & -0.05220 & 0.0 \\ 0.0 & 0.0 & 1.0 & 0.0 \end{vmatrix} \quad B=\begin{vmatrix} -0.002600 \\ 0.0 \\ 0.003260 \\ 0.0 \end{vmatrix}$$

2. Approach-2: flap down (20 deg.), U=56.6 m/sec

$$A=\begin{vmatrix} -0.001770 & -0.05414 & 0.001765 & 0.0 \\ 0.0 & 1.0 & 0.0 & 0.0 \\ 0.05287 & 0.06787 & -0.05332 & 0.0 \\ 0.0 & 0.0 & 1.0 & 0.0 \end{vmatrix} \quad B=\begin{vmatrix} -0.002607 \\ 0.0 \\ 0.003268 \\ 0.0 \end{vmatrix}$$

3. Wave off: flap up, U=77.7 m/sec

$$A=\begin{vmatrix} -0.001834 & -0.04906 & 0.001838 & 0.0 \\ 0.0 & 1.0 & 0.0 & 0.0 \\ 0.04797 & 0.06151 & -0.04734 & 0.0 \\ 0.0 & 0.0 & 1.0 & 0.0 \end{vmatrix} \quad B=\begin{vmatrix} -0.002624 \\ 0.0 \\ 0.003290 \\ 0.0 \end{vmatrix}$$

$$|b_{31}|\ll 1 \tag{4-23}$$

On the other hand, as for this prolbem, the jump condition of the maximum principle is applicable in principle, because the maximum principle considers the arbitrary variations at the entry point unlikely to the TPO method. However, it is very troublesome in practice to obtain the numerical solutions for many cases by the maximum principle when the optimal entry point changes its location in state space according to the final time change such as the case of the angle of attack

constraint for the aircraft.

Consequently, it is extremely difficult to treat the problem exactly in any numerical sense for the investigators who want to know the effect of angle of attack constraint on the width of the controllable region. The relation between angle of attack and control constraint is inquired hereafter to lead the simplifications in calculation.

We presume, from the nature of constraint and of optimal trajectory without state constraint, that the optimal trajectory can be paritioned into following three types:

I. $u_{\min} \geqq u_{\min 1}$
Control quantity is too small to violate the angle of attack constraint.

II. $u_{\min 1} \geqq u_{\min} \geqq u_{\min 2}$
Aircraft can move along the angle of attack constraint boundary at once without violation in any time. It can be solved by the TPO method.

III. $u_{\min 2} \geqq u_{\min} \geqq u_{\min 3}$
Pilot of an aircraft is required to take counter control stick movement for a moment just before the entry point to the constraint boundary. It is difficult to treat in this case.

wherein $u_{\min 1}$ denotes the elevator angles that coincides with the ones giving angle of attack constraint in steady state, and $u_{\min 2}$ denotes the critical elevator angle below which is can no longer move along the constraint boundary at once, and $u_{\min 3}$ denotes the absolute minimum elevator angle determined from the horizontal tail stall or mechanical limits.

In Fig. 4–5, these circumstances are shown. From this figure, it is understood that in type II or III, the time interval of the control $u_{\min 3}$ is comparatively short to the total flight time, because this interval apparently depends on the aircraft response time. Therefore, the effect of control in this interval is considered to be not so large when the considering flight time is sufficiently long. In this paper, taking the assumption that the condition

$$u_{\min} = u_{\min 1} \tag{4–24}$$

is held, we would treat this case exactly and investigate the effect of angle of attack constraint on the width of the controllable region qualitatively. The value of $u_{\min 1}$ is determined by executing several calculations of state-free-height-minimization.

4–3 Lower Boundary of the Controllable Height

4–3–1 Without Thinking of Presence of the Ground

The problem, in which the presence of the ground is not considered without touch down point, is the simplest case and corresponding to the case for the airport on some plateau. This case is prefered first because this contains the fundamental numerical procedures needed also in the problem including the constraint of presence of the ground. The performance index is

$$\max.\ x^0 = x_4(t_f). \tag{4-25}$$

A trajectory corresponds to a point on the lower boundary of the controllable height region for the same example as the one in 4–2–1 is obtained by the TPO method and is shown in Fig. 4–6.

4–3–2 Presence of the Ground

When the ground exists, we can no longer simply translate the optimal trajectory in parallel as stated in section 4–2. We must, accordingly, reformulate the problem in another way to treat analytically. This is, however, considered to be difficult problem. To proceed on our way of investigation, we are to depend on rather numerical approach in this study for this problem; if some point can not be clarified by analysis, we are to try to make it plain with the aid of many numerical calculations.

As a matter of convenience for the discussions in the following paragraphs, we call the optimal trajectory as A-type which has contacted with the ground surface already before it reaches the specified final touch down point and call the another

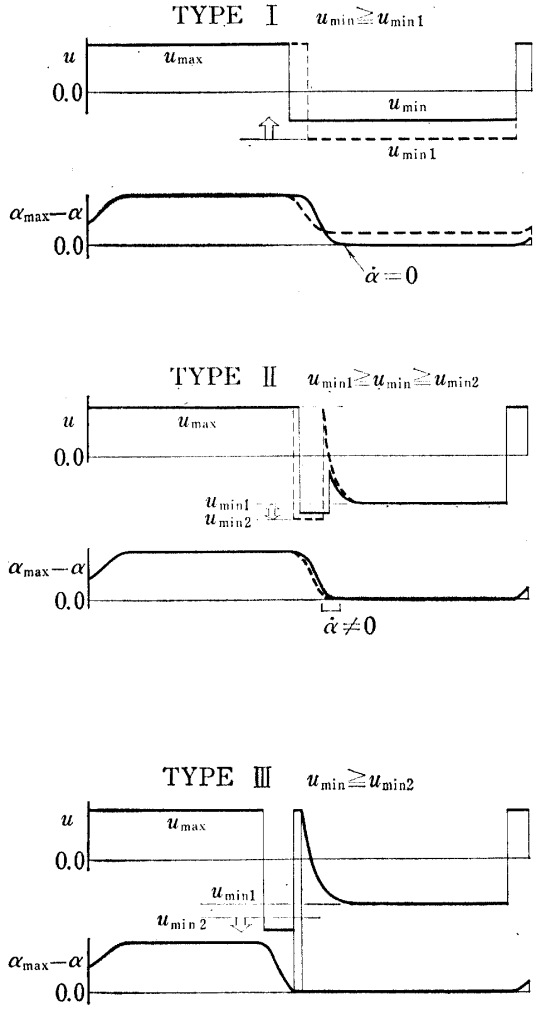

FIG. 4–5. Classification of optimal solution with respect to control limit

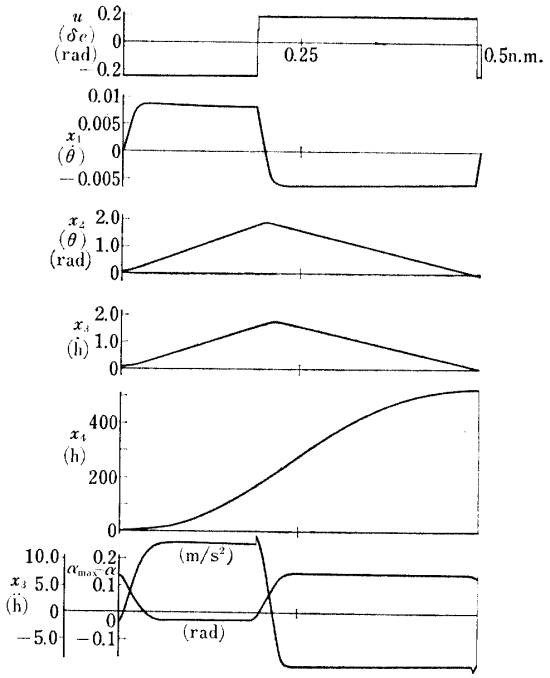

FIG, 4–6. Optimal control and trajectories for minimum initial height: aircraft-1, approach-2, U=49.9 m/s, $\gamma_0=\Theta_0=-2.5$ deg., $-0.255 \leqq \delta_e \leqq 0.195$

optimal trajectory as B-type which has not touched the ground surface except at the touch down.

I. A-Type Optimal Trajectory

A given final time is denoted by t_f and the optimal trajectory until the point of contact to the ground surface is by S_1. The remainder part of the optimal solution is denoted by S_2. S_1 trajectory satisfies the following conditions at contact point:

$$h=0 \tag{4-26}$$

$$\dot{h}=0 \tag{4-27}$$

In this place, let θ_J be the pitch angle of the aircraft at this contact point and $h_{\min}$ be a point on the lower boundary of the controllable height region with the presence of the ground. If the initial condition x_0, final conditions x_f and t_f are given, then $h_{\min}$ is represented reasonably as

$$h_{\min}=h_{\min}(x_0, x_f, t_f). \tag{4-28}$$

Further, when x_0 and x_f do not change, $h_{\min}$ can be regarded as function of t_f as follows:

$$h_{\min}=h_{\min}(t_f) \tag{4-29}$$

Hence this case has a singular nature that some times the optimal solution is not determined uniquely as will be shown in later, we add new variable θ_J which shows the aircraft attitude at the contact point as a parameter designating the contact condition, and we would try to discuss numerically about the relation among $h_{\min}$, θ_J and t_f.

I–1. Sufficiently Large t_f

When there is a sufficient distance to the touch down point, $h_{\min}$ can be obtained by next proposition:

(Proposition)

Let S_1^* be the optimal trajectory satisfying $h=\dot{h}=0$ at t_f and having min. height loss nature, and let S_2 be the proper trajectory satisfying the given final conditions and initiating from the end point of S_1^*. If there exist S_2^* and S_2, the initial height of S_1^* is a point on the lower boundary of the controllable height region.

(Proof)

Let a trajectory S_3 exists, which has less initial height than that of $S_1^*+S_2$. Since this trajectory must be contact with the ground (A–type is assumed), a sub-trajectory S_1 which is a segment of S_3 before the contact point, having less height loss than S_1^* must exist. This contradicts the assumption. Q.E.D.

The trajectory S_1^* and S_2 can be calculated as below: S_1^* is a solution of the maximum height problem in order time. This corresponds originally to the minimum height loss trajectory to $\dot{h}=0$ of the final-time-free problem.

Since the time free problem can not be treated directly by the TPO method, many maximum height problems with different final time t_f must be calculated in order to

find the optimal final time. Calculated example is shown in Fig. 4–7 for the case of aircraft–1, approach–2 and $\gamma_0 = -2.5$ deg. Thick solid line indicates the trajectory S_2 is required only to translate the aircraft from height zero to touch down point and is not required any optimality. Using Sinnott's method, this is easily constructed. S_2 is calculated based on S_1^* and is shown in Fig. 4–8. We call these trajectories as A–I trajectory.

The total flight time t_f is expressed by

$$t_f = t_{f1} + t_{f2}. \tag{4–30}$$

Let us consider that the total flight time t_f becomes gradually short. We should use

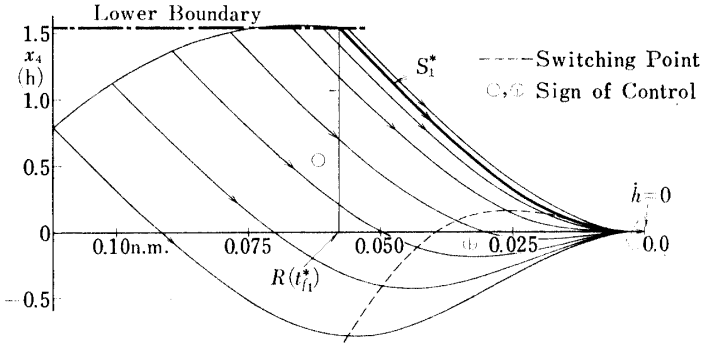

FIG. 4–7. Optimal trajectories which enter into ground tangentially and give maximum initial height: aircraft–1, approach–2, $\gamma_0 = \Theta_0 = -2.5$ deg., $|\delta_e| \leqq 0.055$, R≦1/9 n.m.

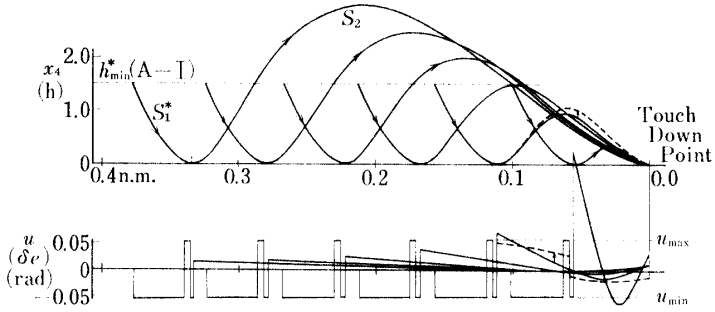

FIG. 4–8. Matching of optimal trajectory S_1^* and suitable trajectory S_2: aircraft–1, approach–2, $\gamma_0 = \Theta_0 = -2.5$ deg., $|\delta_e| \leqq 0.055$

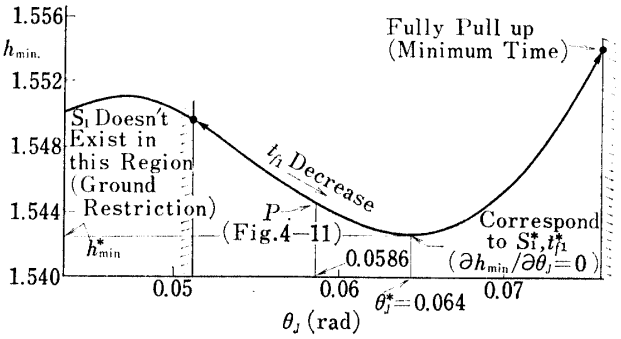

FIG. 4–9. Relation of θ_J and $h_{\min}$ which gives S_1: aircraft–1, approach–2, $\gamma_0 = -2.5$ deg., $h(t_f) = 0.0$, $|\delta_e| \leqq 0.055$

S_1^* as the optimal subarc if it is possible to exist. However, since t_{f1} is determined independently to t_f, the length of t_{f2} should be adjusted to that of t_f. As clearly indicated in Fig. 4–8, it becomes more and more difficult to construct the trajectory S_2 within the limit of the given control constraints when the length of t_{f2} becomes short. From this fact, we can presume that it becomes impossible to construct trajectory S_2 when t_f is smaller than some critical value t_f^*. Physical explanation may be described as below:

It becomes difficult for the aircraft to keep the floating inclination in less than time interval t_f because of the excessive pitching attitude θ_J at the end of S_1^*. The solution of maximum and minimum heights, which are solved with the initial condition of S_1^* value and with final time t_f as parameters, are shown in Fig. 4–9 for aircraft–1, approach–2 and $\gamma_0 = -2.5$ deg. The above mentioned discussions are supported numerically by the fact that the region bounded with shaded line allows us the existence of S_2.

I–2. $t_f < t_f^*$

When t_f becomes smaller than t_f^*, it is no longer possible to contain S_1^* in the optimal trajectory. Also, since even in this case, sub-trajectory S_1 must be optimal, S_1 must be one of the trajectories which have a final attitude θ_J on the $h_{\min}$ curve of Fig. 4–9. If we try to solve this problem, it seems to be necessary to employ the procedure described in the following paragraph:

We choose a suitable point on $h_{\min}$ curve of Fig. 4–9, then S_1 and the final values are determined and also t_{f1} is determined at the same time. Taking the final time t_{f2} as a parameter, maximum and minimum height problems should be solved to obtain the reachable region and to obtain the time t_{f2}^* which corresponds to the zero height point of the boundary of reachable region (Fig. 4–10A).

We can ascertain at least that for time interval $t_f \geqq t_{f1} + t_{f2}^*$, the aircraft can be controlled to the designated point from the selected height $h_{\min}$, because the optimal trajectory containing S_1 as the sub-trajectory and satisfying all restrictions are reasonable in $t_f \geqq t_{f1} + t_{f2}^*$ (Fig. 4–10B). Doing above calculations for all points on $h_{\min}$ curve of Fig. 4–9 or for all of S_1, the lowest boundary of height for the arbitrary time t_f being less than t_f^* can be constructed from the calculated set of sub-optimal points on height-time plane (Fig. 4–10C). Let a trajectory on the lowest boundary be A–II.

By the way, it is difficult in number of calculations to execute the above mentioned procedures. In this study, we are rather interested in the range of existence of the A-II trajectories than the strict solution, so it seems to be adequate to consider like following:

Choosing a point on $h_{\min}$ curve of Fig. 4–9 as a initial condition of S_2 and solving the maximum and minimum height problems with respect to many t_{f2}, we can obtain the results similar to Fig. 4–11. In this figure, at the region of $R > R'$, true height boundary must be lower than $h_{\min}$ because $h_{\min}$ guarantees the safe landings in $R > R'$. On the other hand, it is evident that any control can not realize the safe landings from the lower height than $h_{\min}^*$ which is initial height of S_1^*. So, the true

minimum height is greater than h^*_{him}. The region surrounded by shaded boundary shows the one which contains the minimum height. The range of this region is only 5 cm in real scale. We think there is no technological avantages to discuss further about the solution A–II.

II. B-Type Optimal Trajectory

When the final time t_f becomes sufficiently small, it is not necessary to consider the effect of presence of the ground because it becomes possible to get as the solution of maximum height problem the optimal trajectories which no longer contact with the ground surface before touch down.

The lower boundary of the controllable height and its range are calculated about

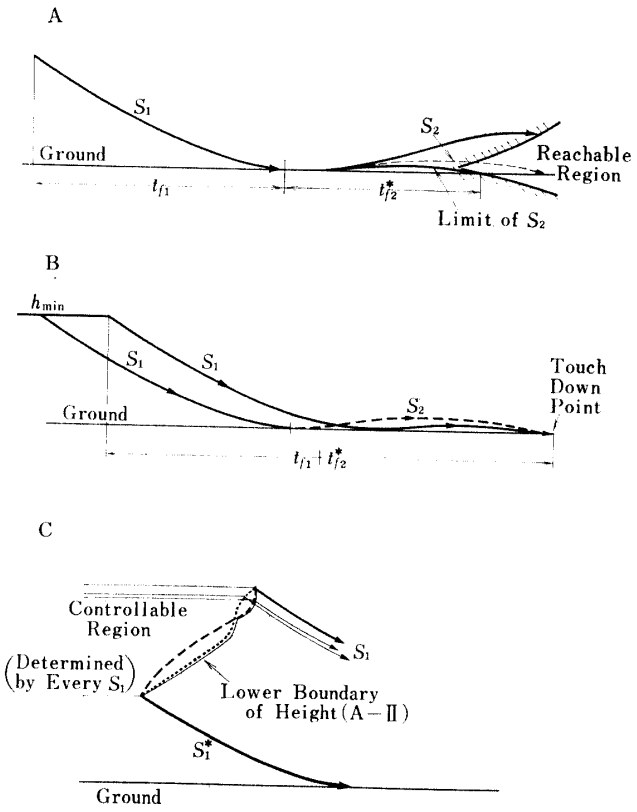

Fig. 4–10. Explanation diagram of getting the A–II type lower height boundaary

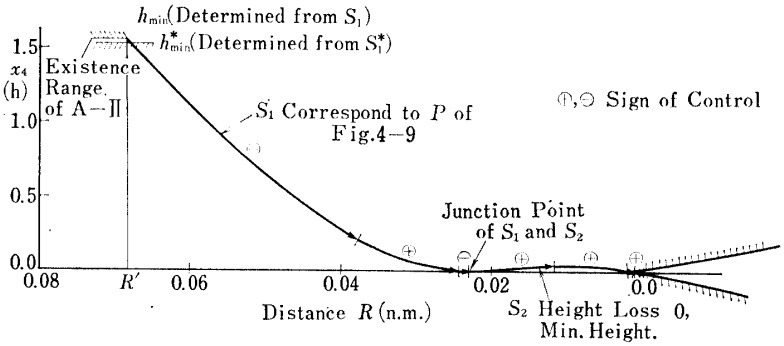

FIG. 11. Existence range of A–II optimal trajectory: aircraft–1, approach–2, $\gamma_0=-2.5$, deg., $\theta_J=0.0586$, $|\delta_e|\leqq 0.055$

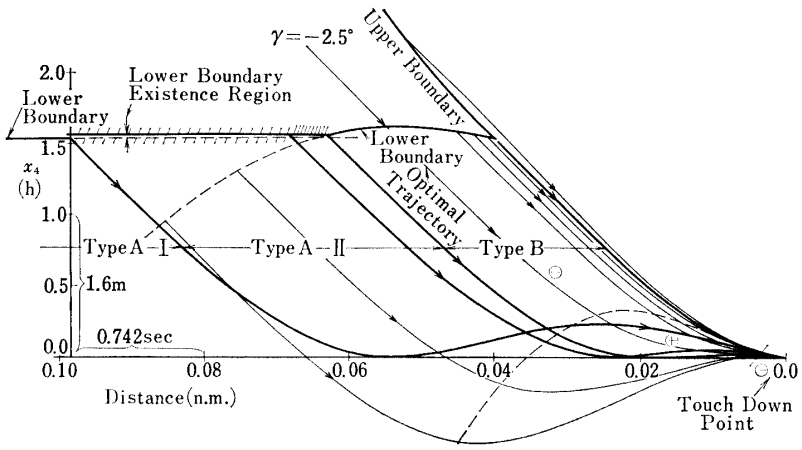

FIG. 4–12. Upper and lower height bonndary and corresponding trajectories: aircraft–1, approach–2, $\gamma_0=-2.5$ deg., $|\delta_e|\leqq 0.055$

those aforementioned trajectories of A-I, A-II and B types and are shown in Fig. 4–12. In spite of the different meanings of those three types and of the necessity of nuisance calculations, the lower limit of the controllable height does not have the notable differences among them. Consequently, it seems reasonable to regard the lower boundary of the controllable height region as constant in height.

4–3–3 Angle of Attack and Attitude Constraint

Pitching angle is not so severe in this case, and the angle of attack constraint should be treated by the approximate method like the one used to get the upper height boundaries.

5. CONTROLLABLE HEIGHT AND SAFE LANDING

In this section, we show firstly the state of the calculated controllable height boundaries of a conventional aircraft in spot landing. There also shown the effects of the some approach condition such as approach angle or velocity on the width of controllable height region. The landings from wider controllable region evidently bring us higher degree of safety and reliability. Accordingly, it is considered to be meaningful to know the relation between these regions and conditions.

Secondly, based on the calculated controllable height regions, we discuss the desirable control method or approach paths from the view point of safety. A medium size turboprop transport aircraft is chosen as a model all over the numerical calculations. The method illustrated in details in section 4 is used to obtain the controllable height region of the aircraft.

5–1 Effect of Parameters on Controllable Height Region

5–1–1 Controllable Height Region with Elevator Constraint

We consider the transportation of passengers. We take the elevator angle constraint which gives rather narrow vertical acceleration limit such as

$$|\ddot{h}|\leqq 0.3g \tag{5–1}$$

Several numerical trials make us sure that the corresponding elevator angle constraint to the above numerals is

$$|u| \leqq 0.055 \tag{5-2}$$

I. Controllable Height Regions for Rather Long Time Flight

The calculated controllable height regions under the constraint of Eq. 5–2 for 1.0 naut mile are shown in Figs. 5–1~5–3. In these figures, abccisa shows the ground surface and solid lines show the lower and upper boundaries of controllable height in which the lower one under the presence of the ground is parallel to the ground surface. Broken lines indicate the optimal trajectories from the upper and lower height boundaries.

Fig. 5–4 illustrates the variational control and state variables. The results of above calculations bring us followings:

1. When the aircraft is far from the touch down point, the controllable height region is very wide.
2. When the ground exists, the steeper descent path presents the wider controllable height regions.
3. Irrespective of the approach distances, the controls which give upper and

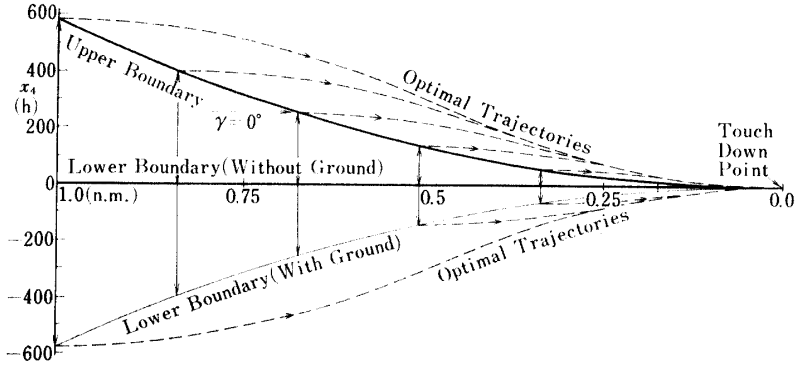

FIG. 5–1. Controllable height boundary and corresponding trajectories for $\gamma_0 = 0.0$ deg.: aircraft-1, approach-2, $U = 49.9$ m/s, $|\delta_e| \leqq 0.055$, $h(t_f) = -0.3$ m/s (continued)

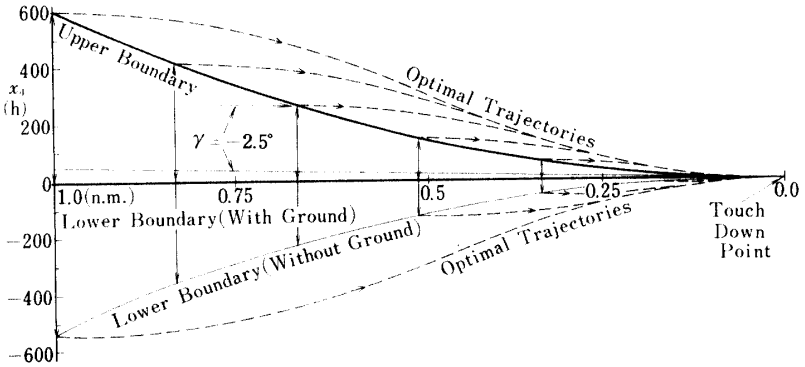

FIG. 5–2. Controllable height boundary and corresponding trajectories for $\gamma_0 = -2.5$ deg. (continued)

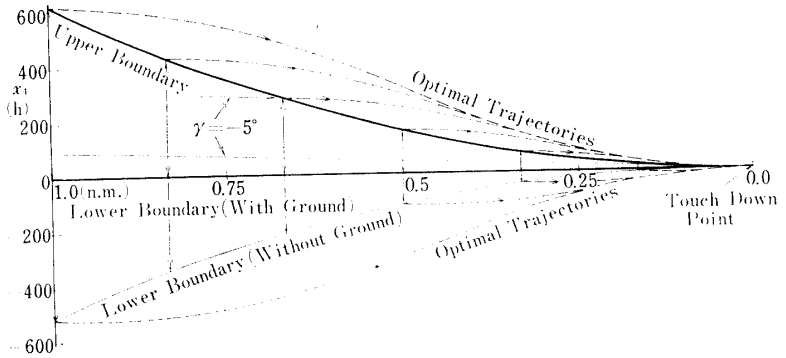

FIG. 5–3. Controllable height boundary and corresponding trajectories for $\gamma_0 = -5.0$ deg. (concluded)

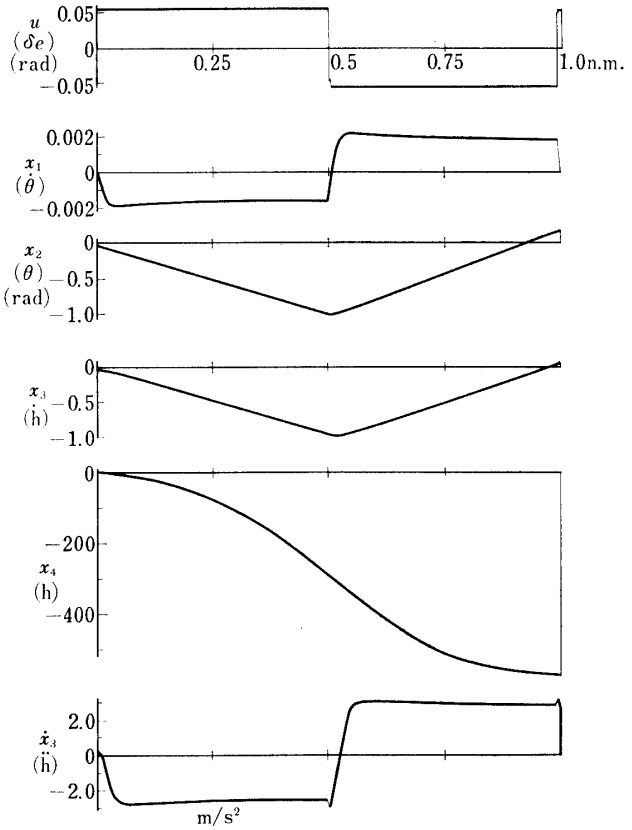

FIG. 5–4. Optimal control trajectories for for upper height boundary: aircraft–1, approach–2, $U = 49.9$ m/s, $\gamma_0 = \Theta_0 = -2.5$ deg., $|\delta_e| \leqq 0.055$, $R \leqq 1.0$ n.m.

lower height region have same patterns.

Now, only next restriction is provided as the final condition in optimization.

$$\dot{h} = -0.3 m/s \tag{5–3}$$

Therefore, whether the other state quantities such as pitch angle or pitch rate of the aircraft violate the ordinary value or not should be made certain. Final pitch angles and pitch rates in the optimal trajectories are plotted in Fig. 5–5. This figure means that the model aircraft, controlled so as to maximize or minimize the

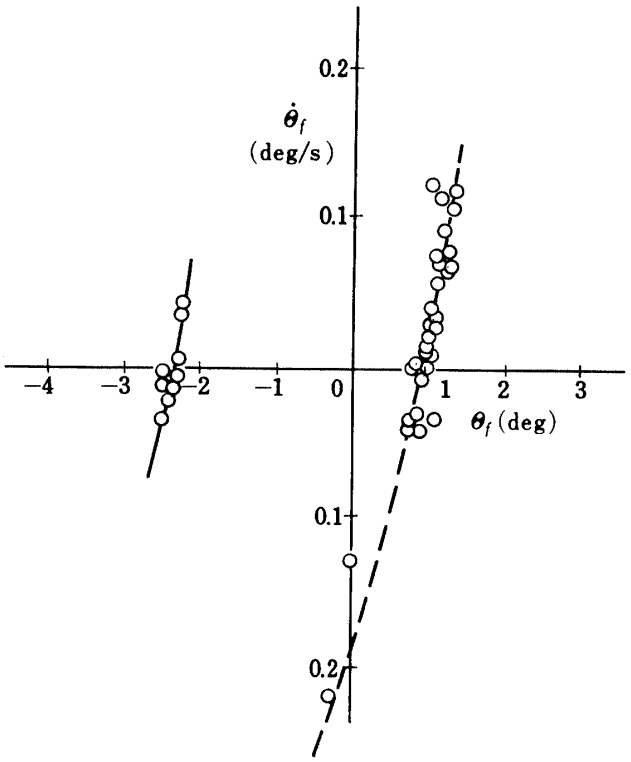

FIG. 5–5. Aircraft attitude and its rate of change at the touch down point: aircraft-1, $\gamma_0=0.0\sim-5.0$ deg., $R\leqq 1.0$ n.m., $|\delta_e|\leqq 0.055$

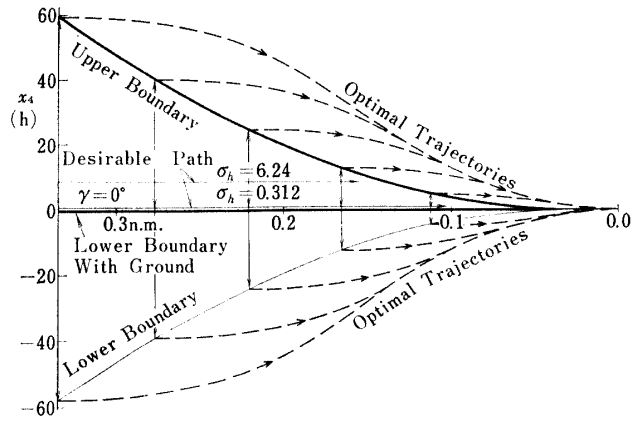

FIG. 5–6. Controllable height boundary and corresponding trajectories for $\gamma_0=0.0$ deg. and $R=1/3$ n.m.: aircraft-1, approach-2, $U=49.9$ m/s, $|\delta_e|\leqq 0.55$, $\dot{h}(t_f)=-0.3$ m/s (continued)

initial height keeping attention only to final rate of descent, is attended with good attitude and pitch rate results. In this sense, the model aircraft adopted in this study seems to have good control characteristics.

II. Controllable Height Regions for Short Time Flight

The calculated results of controllable height boundaries for relatively short flight distance of 1/3 naut mile are shown in Figs. 5–6~5–8. These figures show that the controllable region for shallower approach path has wider bound, namely, the controllable height region of −2.5 deg. approach path is wider than that of −5.0

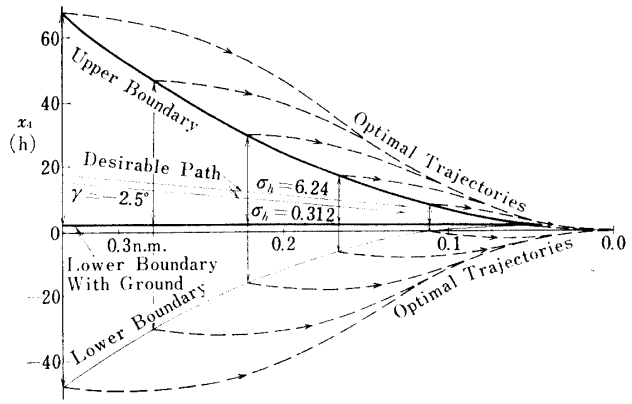

FIG. 5–7. Controllable height bonndary and corresponding trajectries for $\gamma_0=-2.5$ deg. and $R=1/3$ n.m. (continued)

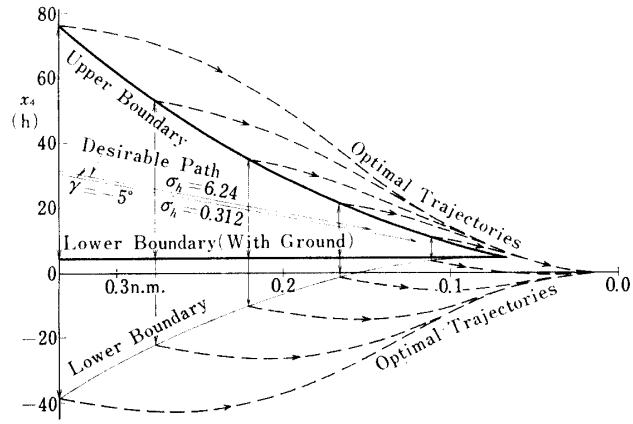

FIG. 5–8. Controllable height boundary and corresponding trajectories for $\gamma_0=-5.0$ deg. and $R=1/3$ n.m. (concluded)

deg. path when the approach distance is less than 1/9 naut mile. Fig. 5–8 shows also that in case of steep approach like $\gamma_0=-5.0$ deg., the controllable height region diminishes before the touch down point. This means the necessity of flare maneuver that compells the aircraft to more shallow path and elongate the controllable region. More details of the controllable region for $\gamma_0=-2.5$ deg. are shown in Fig. 4–12 in previous section.

5–1–2 Effect of the Attitude Constraint

The optimal trajectories from the boundary of controllable height region for

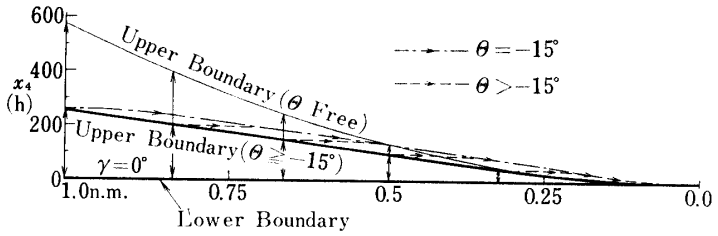

FIG. 5–9. Controllable height boundary with attitude constraint for $\gamma_0=0.0$ deg.: aircraft-1, approach-2, $U=49.9$ m/s, $|\delta_e|\leqq 0.055$, $h(t_f)=-0.3$ m/s (continued)

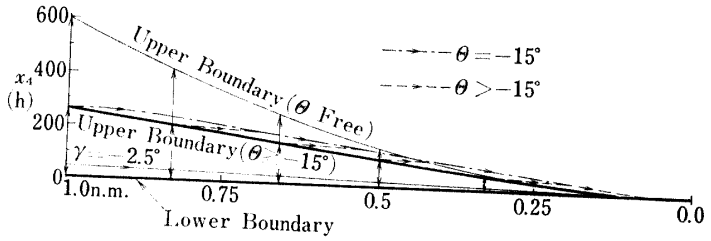

FIG. 5-10. Controllable height boundary with attitude constraint for $\gamma_0=-2.5$ deg. (continued)

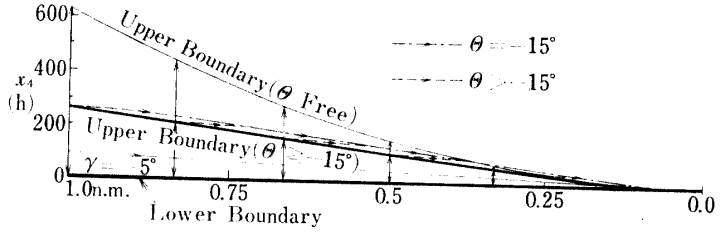

FIG. 5-11. Controllable height boundary with attitude constraint for $\gamma_0=-5.0$ deg. (concluded)

the elevator angle constraint of Eq. 5–2 have fairly margins for the wing stall, but the optimal trajectory for the upper boundaries of controllable height region gives extremely large attitude if the approach path becomes long. Such attitude as $\Theta=-45$ deg. should not be allowed especially in passenger transportations. Therefore, it is necessary to obtain the controllable height regions with favorable attitude constraint. The method of obtaining the controllable height region for this case is already shown in 4–2–2. As the long time nose down control means the crash of aircraft into the ground, the optimal trajectories giving lower boundary of controllable height region do not violate the attitude constraint by the presence of the ground. The results of the numerical calculations for the controllable height boundaries for the constraint of

$$\Theta \geqq -15° \tag{5-4}$$

are shown in Figs. 5–9~5–11. Fine solid lines indicate the controllable regions without the attitude constraint for comparison. Optimal trajectories are shown by the broken lines and chain lines. The optimal control history from the upper boundary is shown in Fig. 4–4 in previous section.

As might have been expected, the height of upper boundary of the controllable region decreases considerably because of the attitude limit, and the most conspicious point is the linear variation of the upper boundaries with respect to the distance from touch down point.

5–1–3 Effect of Characteristics of Aircraft

1. Effect of Flight Phases in Approach

The typical flight phases in landing of aircraft-1 are phase-2, phase-1 and wave off. Differences of dynamic characteristics are shown below using natural frequency ω_n and damping ratio ζ.

phase–1: $\omega_n^2=0.00398$, $\zeta=0.858$
phase–2: $\omega_n^2=0.00453$, $\zeta=0.798$
wave off: $\omega_n^2=0.00405$, $\zeta=0.758$

Controllable height regions of each phase for less than 1/3 naut mile distance are shown in Fig. 5–12 for the same control constraint. This figure shows that the differences of flight phase affect little the controllable regions or optimal control laws.

2. Effect of Difference of Aircraft

To assure the effect of difference of aircraft, the upper boundary of the controllable region for aircraft-2 (Table 2) whose damping ratio ζ is equal to 0.5 is calculated. The initial flight path angle is -2.5 deg. and the initial distance from

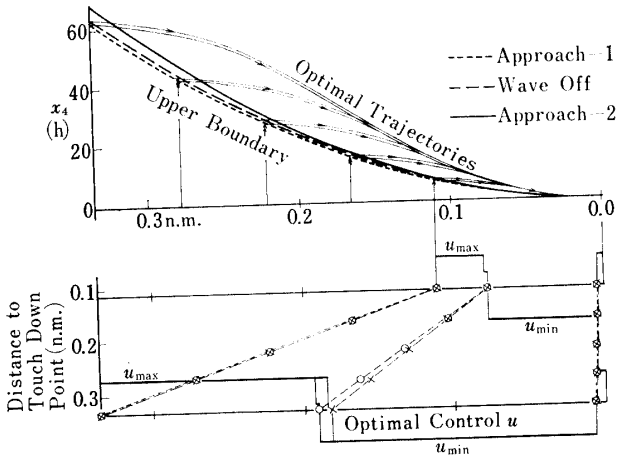

FIG. 5–12. Effect of flight phases in approach: aircraft–1, $U=49.9$ m/s, $|\delta_e|\leqq 0.055$, $\gamma_0=-2.5$ deg.

TABLE 2. Coefficient Matrices of Equation of Motion of Aircraft–2

$$A=\begin{vmatrix} -0.76 & -0.6 & 0.01277 & 0.0 \\ 0.0 & 1.0 & 0.0 & 0.0 \\ 31.0 & 0.0 & -0.4 & 0.0 \\ 0.0 & 0.0 & 1.0 & 0.0 \end{vmatrix} \qquad B=\begin{vmatrix} -2.375 \\ 0.0 \\ 1.0 \\ 0.0 \end{vmatrix}$$

TABLE 3. Approach speeds and trimmed angle of attack

U (m/s)	α (rad)	α (deg)
52.5	0.05114	2.93
49.9	0.07464	4.28
47.5	0.09984	5.72
45.0	0.1312	7.52
42.5	0.1644	9.42
40.0	0.2099	12.03

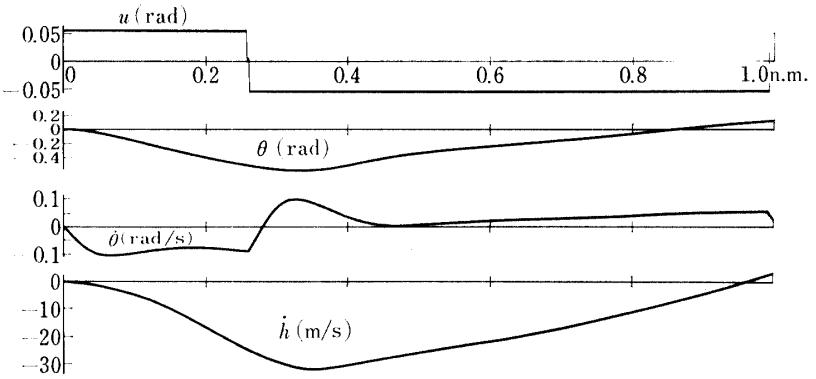

FIG. 5–13. Optimal control and trajectories giving upper height boundary for aircraft-2: $\gamma_0=-2.5$ deg., $R=1.0$ n.m.

the touch down point is 1.0 naut mile (Fig. 5–13). It is recognized that the control pattern of aircraft-2 is similar to aircraft-1 in spite of its smaller damping ratio. It is worth noting that in this case the terminal attitude becomes over 10.0 deg. This means that as for the aircraft-2 the terminal attiutde constraint is required in optimization procedure to accomplish the safe landing, and therefore, this necessarily means that the controls from critical condition are more difficult than that of aircraft-1.

5–1–4 Approach Speed and Controllable Height Region

It is needless to say that the wider controllable region leads aircraft to rather safer landings if the flying quality of the aircraft is not changed. The purpose of this subsection is to make clear the effect of approach speed on controllable height region with the constraints of angle of attack, control quantity and vertical acceleration. It should be noted that the controllable region of aircraft at rather short distance from the specified touch down point is an issue in this case, for the width of the controllable height region is important around there for landing controls.

I. Angle of Attack Constraint

Low speed steady state condition needs high trimmed angle of attack. When trimmed angle of attack is too large, the margin of angle of attack to stall is small and it is unable to pull fully up the aircraft. Accordingly, it is expected that the restriction of stall in the low speed approach makes the controllable height region rather narrower.

Now, the reference state satisfies the relation

$$L \fallingdotseq W \cos\gamma \tag{5–5}$$

Substituting next relations to above,

$$L=\frac{1}{2}\rho U^2 S C_L \tag{5–6}$$

$$C_L=C_{L_0}+a\alpha \tag{5–7}$$

we get the following trimmed angle of attack equation:

TABLE 4. Angle of attack and corresponding aerodynamic derivatives

α (deg)	C_{L_0}	C_{D_0}	$C_{D\alpha}$	C_{m_0}
2.93	1.375	0.132	0.6647	−0.045
4.28	1.52	0.147	0.6647	−0.070
5.72	1.67	0.162	0.6647	−0.090
7.52	1.86	0.180	0.6647	−0.130
9.42	2.065	0.201	0.6647	−0.165
12.03	2.345	0.240	0.6647	−0.210

$$\alpha=\frac{1}{a}\left(\frac{W\cos\gamma}{(1/2)\rho S}\frac{1}{U^2}-C_{L_0}\right) \tag{5-8}$$

From this relation, we can calculate the angle of attack corresponding to the specified steady flight velocity U and flight path angle γ. Calculated angles of attack for $\gamma=-2.5$ deg. with parameter U are shown in Table 3. Aerodynamic derivatives for the trimmed angle of attack are estimated from wind tunnel test data and are shown in Table 4. The optimization of initial height can be done according to the procedures described in 4–2–3, and the results for $\gamma_0=-2.5$ deg., R=1/3 naut mile, $u_{\max}=0.11$ and $\alpha_{\max}=12.0$ deg. are shown in Fig. 5–14. This figure shows the relation between elevator controls and angle of attack in the trajectories from upper height boundaries with the parameter of approach speed U. As the velocity decreases, we are noticed as expectedly that it becomes impossible to pull large amount of control stick and the pilot is unwillingly obliged to continue to pull small amount of stick for long time.

II. Control Constraint

If the control limit is determined from the mechanical limitation only, the width of the controllable height regions at a specified point do not depend on the approach velocities. This is evident from the fact that the equation of motion is governed by nondimensional time $\hat{t}$, and that the nondimensional time $\hat{t}$, real time t (sec) and flight velocity U (m/sec) has the following relation.

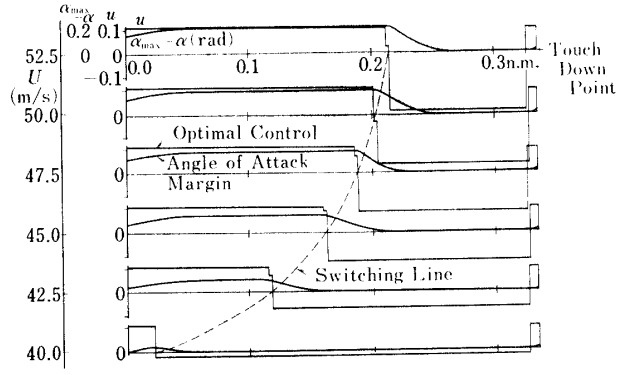

FIG. 5–14. Relation between approach velocity U and controls giving upper height boundary: aircraft-1, approach-2, $\gamma_0=-2.5$ deg., $u=0.11$, $\alpha_{\max}=12$ deg.

$$\hat{t}=\frac{2Ut}{\bar{c}} \tag{5-9}$$

III. Acceleration Limit

Since the relations between dimensional and nondimensional variables are

$$h=\frac{2\boldsymbol{h}}{\bar{c}}, \quad \tau=\frac{\bar{c}}{2U}, \quad \hat{t}=\frac{t}{\bar{c}}, \tag{5-10}$$

where $\boldsymbol{h}$=[m], t=[sec], U=[m/sec], we have the next relations about nondimensional rate of ascent and acceleration:

$$x_3=\frac{dh}{d\hat{t}}=\frac{1}{U}\frac{d\boldsymbol{h}}{dt}, \quad \dot{x}_3=\frac{d^2h}{d\hat{t}^2}=\frac{\bar{c}}{2U^2}\frac{d^2\boldsymbol{h}}{dt^2}. \tag{5-11}$$

From these relations, we can understand that under the same quantity of control constraint, the greater the approach speed, the greater the variational normal accelaration. Inversely to say, the same accelaration constraint needs the different control limits according to each approach velocities. We can obtain the contours of height boundaries for some variational acceleration limits in the phase plane of U and h, because we can calculate from Eq. 5–11 the steady variational acceleration in the nondimensional space using the optimal trajectories for several control limits and approach velocities.

Consequently, from the discussion above, we can anticipate that the controllable height region becomes narrow at low approach speed region due to the angle of attack limit and becomes also narrow at high approach speed due to the accelaration limit and that the controllable region is restricted within some constantly spreaded range because of the presence of the absolute control quantity restriction. If these relations can be determined quantitatively for each aircraft, controllers or pilots of aircraft can choose approach velocity which represents the most wide controllable height region.

The calculated results for controllable height regions taking into account these limitations are shown in Fig. 5–15. The flight phase is approach-2 and the flight path angles are 0~−2.5 deg. and the considering flight distance is 1/3 naut mile. The controllable height boundaries under the circumstances of $\gamma_0=-2.5$ deg., $u\leqq 0.11$ and $|\dot{x}_3|\leqq 0.5\,g$ are shown by thick solid lines. The velocity range giving the widest controllable region is $1.125\sim 1.175\,V_s$ for the aircraft-1. As a rule, the approach velocity giving the widest controllable region increases when the absolute value of allowable control quantity increases. Of course, if we consider only the wing stall constraint, the controllable region becomes monotonously wider as the result of increasing of the approach velocity.

It should be noted that the relative relations between the approach velocities and the controllable height region are not so affected by approach angles. This suggests that the desirable approach velocity could be determined independently to the approach angles.

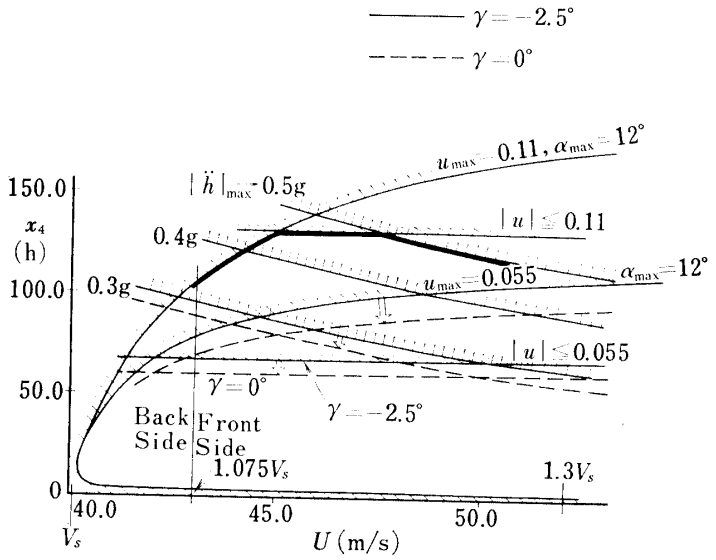

FIG. 5–15. Controllable height regions related to approach velocity, acceleration limits and control limits: aircraft–1, approach–2, $\gamma_0=-2.5$ deg., $\alpha_{max}=12$ deg., $R=1/3$ n.m.

5–2 *Controllable Height Region and Safe Landings*

In this section, a discussion for the desirable approach angle with respect to safe landings is tried on the bases of the results of previous section.

5–2–1 *Flight Patterns in Approach and Landing*

In the automatic landing systems in practical use, the following approach and landing patterns are used [*29, 30*]: Above 100 ft height, an aircraft can track the glide path signal correctly, and approaches along the given glide path. In the region of 100~60 ft height, the aircraft is commanded to maintain the constant attitude because in this height region the signals of glide path becomes unstable and the radio-altimeter is also unstable yet. At the final leg of landing phase below 60 ft height, the aircraft is commanded to execute an exponential flare, and finishes the landing completely. In the manual landing state, simultaneous procedures seem to be taken [*31*]. The approach flight may be broadly divided into steady flight and flare maneuver. As far as the aircraft stays in wide controllable region, the steady flight approach is possible and more over desirable for its easiness and reliableness. On the other hand, when the controllable height region becomes narrower than some threshold width, it is necessary for the aircraft to choose a flight path so that the aircraft belongs to the widest controllable region in each instant. This necessarily leads to flare maneuvers.

And yet, the timing of the commencement of flare is difficult. If it commenced too fast, the time length of unsteady controls becomes too long, which is not desirable from the view point of safety because of the burden of long time precise control. If it commenced too late, the aircraft may probably be out of the controllable regions. This is dangerous.

In the following discussions, the landing pattern are assumed to be constructed

of steady approach and unsteady flare maneuver, and the angles and location of the steady approach path are investigated in view of safety.

5–2–2 Approach Margin and Approach Angle

Proper choice of distance R from the touch down point makes possible to determine t_s that indicates the maximum time length of steady state flight from the specified point (Fig. 5–16). If the distance R is fixed, we can understand that the longer the time length t_s, the shorter the time length of flare. Now, t_s which is related to γ and h is reasonably considered to show one of the measure of safety margin in aircraft landing, for the long t_s means easy control. By the way, it is impossible to realize the specified approach angle γ and height h exactly at the point R. Accordingly, the actual approach angle and heights are presumed to distribute probabilistically around the designated objective value γ_m and h_m. This distribution is considered to be subjected to the influences of the tracking systems, stuff, will or condition of the pilot, the strength of disturbances and commencement time of tracking.

Following assumption is provided here to set forward the investigation.

Assumption: Actual γ and h are in accordance with the normal distribution around γ_m and h_m. The variance from the objective point γ_m and h_m is expressed by σ_γ^2 and σ_h^2.

Using above assumption, we can define a statistical approach margin as

$$M_s=\frac{1}{t_f}t_s(\gamma_m, h_m)P(\gamma, h)d\gamma dh, \tag{5–12}$$

where t_f is flight time from point R and $P(\gamma, h)$ is probability density function.

Here, let us provide a further assumption that

$$\sigma_\gamma^2=0. \tag{5–13}$$

This means that pilots can attain his target perfectly for flight path angle γ, and that the effect of the techniques of the pilots or effect of turbulence on the flight path appears only in variance σ_h^2. It is obvious that to hold the slope of flight path exact is easier than to attain the height exact at some specified point. Approach margin can be rewritten with this assumption as

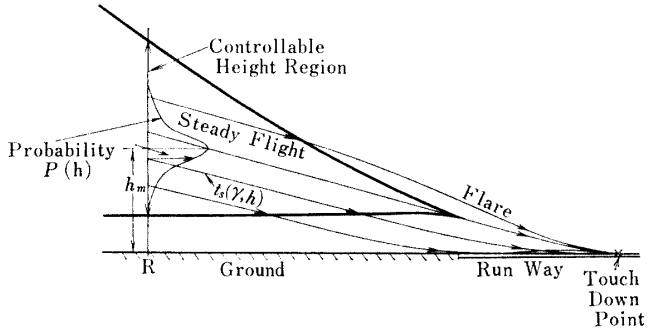

FIG. 5–16. Controllable height region and capable steady approach time t_s

$$M_{s1}=\frac{1}{t_f}\int t_s(\gamma_m, h_m)\frac{1}{\sqrt{2\pi}\,\sigma_h}\exp\left(-\frac{1}{2\sigma_h^2}(h-h_m)\right)dh. \qquad (5\text{–}14)$$

$M_{s1}=1.0$ says that the aircraft can realize the objective flight path with certainty and besides can realize the safe touch down by steady flight only .

Generally, it is expected that the large value of variance σ_h^2 makes M_{s1} small which necessarily means small margins in landings or in approaches. We can calculate the time t_s on the bases of the results of section 5–2–1. The approach margins at distance of R=1/3 naut mile are calculated by using Eq. 5–14 for aircraft-1, approach-2, and are shown in Figs. 5–17~5–19.

In case of $\gamma=0.0$ deg., it is better for approach margins to aim at lower objective height at R=1/3 naut mile if the value of variance σ_h^2 becomes smaller (Fig. 5–17). This tendency goes down with the increase of steepness of approach angles. For instance, in case of $\gamma=-5.0$ deg., the aircraft should aim at height of $h=30$ irrespective of the variance σ_h^2, if it is wanted to make the approach margin maximum (Fig. 5–19).

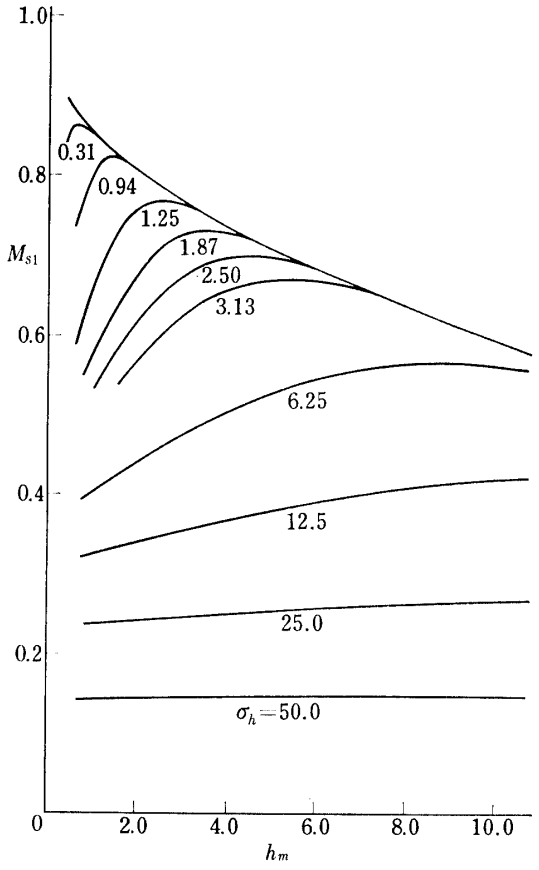

FIG. 5–17. Relation between approach margin M_{s1} and objective height h_m at $R=1/3$ n.m. with respect to standard deviation σ_h: aircraft–1, approach–2, $|\delta_e|\leqq 0.055$, $\gamma_0=0.0$ deg. (continued)

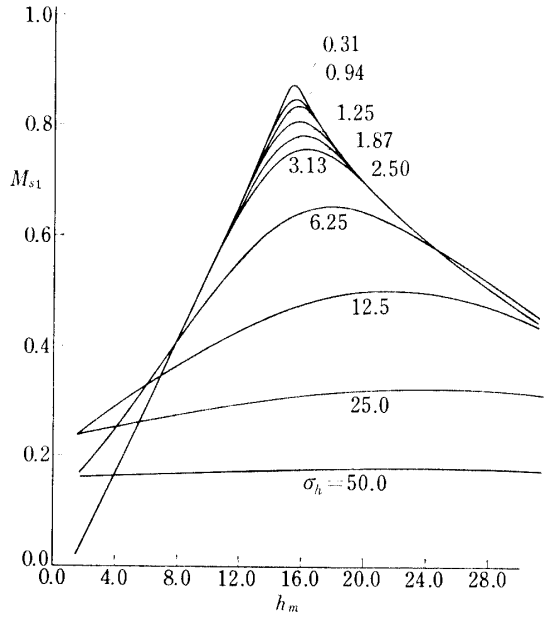

FIG. 5–18. Relation between approach margin M_{s1} and objective height h_m at $R=1/3$ n.m. with respect to standard deviation δ_h:=−2.5 deg. (continued)

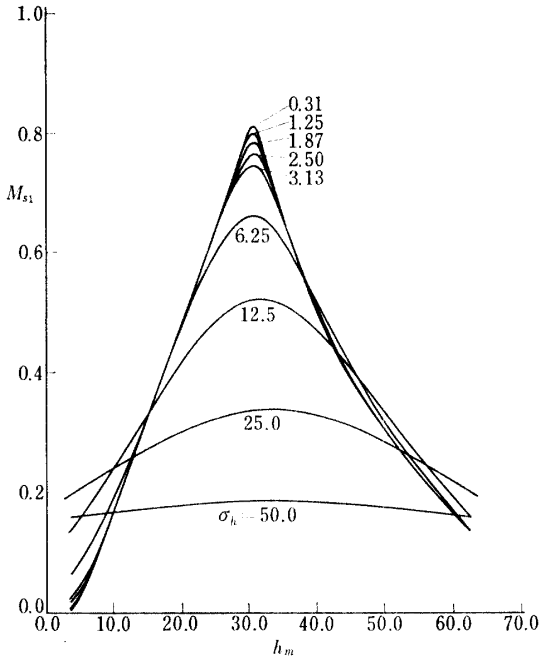

FIG. 5–19. Relation between approach margin M_{s1} and objective height h_m at $R=1/3$ n.m. with respect to standard deviation σ_h: $\gamma_0=-5.0$ deg. (concluded)

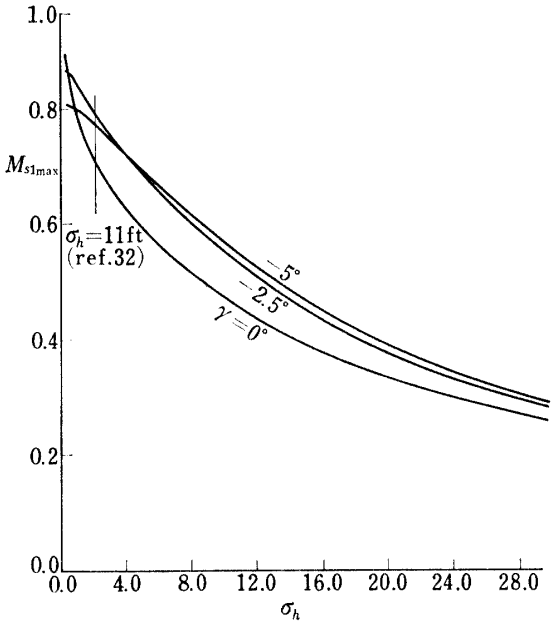

FIG. 5–20. Relation between maximum approach margin M_{s1max} and standard deviation σ_h: aircraft-1, approach-2, $|\delta_e|\leq 0.055$, $R=1/3$ n.m.

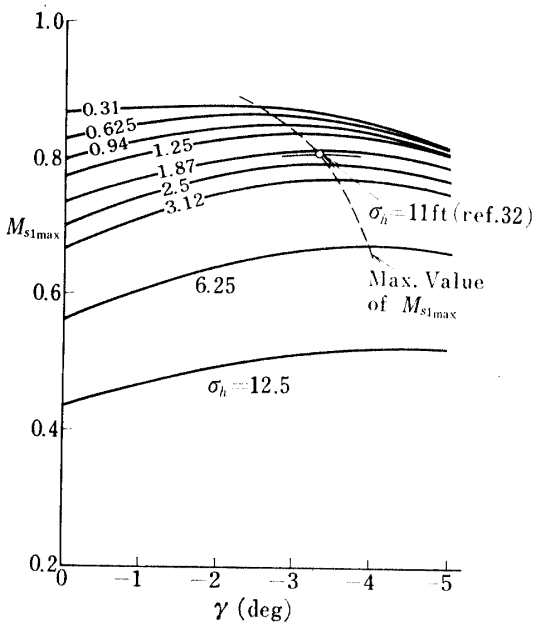

FIG. 5–21. Relation qetween maximum approach margin M_{s1max} and approach angle γ: aircraft-1, approach-2, $|\delta_e|\leq 0.055$, $R=1/3$ n.m.

Further, when the value of σ_h^2 is small, shallower approach angle is, and when large, the steeper approach angle is desirable for the good margins (Figs. 5–17~5–19). In other words, rather shallower approach should be chosen if the aircraft is controlled by a pilot with excellent technique, and rather steeper approach is desirable for the unskillful pilots.

Then from these figures, we can calculate the desirable objective height and corresponding safety margin if the approach angle γ and variance σ_h^2 are determined. Rearrangement of these figures are shown in Figs. 5–20~5–21 in which the maximum value of the approach margin for h_m are indicated on vertical axis. Fig. 5–20 shows that the maximum approach margin decreases abruptly with the increase of variance σ_h^2, and this tendency consists independently to approach angle γ. Fig. 5–21 shows that when the variance σ_h^2 is small in the region of $\gamma=0\sim3.0$ deg., the maximum approach margin is scarcely changed but when the variance becomes large, the maximum margin is considerably changed with respect to approach angle. For example, the approach angle $\gamma=3.0$ deg. gives almost maximum approach margins in any time in the region of $\sigma_h<6$. This feature may also be the theoretical support for the current establishment of the glide slope in ILS. The desirable approach path that are determined from the maximum approach margins corresponding to each variance σ_h^2 for aircraft-1 are obtained and are shown in Figs. 5–6~5–8.

The author considers that these way of thinkings would supply one of the bases of arguments for determination of approach angle of the conventional aircraft. Formerly, the approach angle was determined empirically without any mathematical treatment.

As we have seen, it was made clear that the desirable approach angle in the steady state approach could be determined by the value of variance σ_h^2.

It is worth while to note that in spite of linear equation and large allowable control quantity, the results for approach margin specifically near maximum value are not so different from actuality because in the neighbourhood of the point giving maximum approach margin, the deviation from the steady state is not so large due to the short time application of maximum or minimum control quantities.

6. Conclusion

Two Phases Optimization method based on linear programming is introduced to calculate the controllable height regions of aircraft in landing. This method is confirmed to be sufficiently effective for the problem of obtaining the points of the boundary of controllable region of linear systems. This method is applicable to the problem with first-order state-inequality-constraint.

The controllable height regions for spot landings of aircraft are obtained by using the Two Phases Optimization method under the assumptions that the motion of aircraft is governed by linear equation and is ruled by longitudinal short period mode. It is made clear that the patterns of controls that give the boundary of the controllable region are not affected by the differences of flight phases or dynamic characteristics of the aircraft.

When the attitude limit is added as the constraint, the controllable height region with respect to the spot landings becomes fairly limited compared to the attitude free case. In this case, the controllable height region extends linearly with the

distance from a specified touch down point. Nuisance numerical calculations are needed to obtain the lower boundary of the controllable height region, but the fact that this boundary can be regarded to be constant in height is accertained.

The controllable height region with respect to the spot landings for each approach velocity can be calculated approximately even when the quantities of vertical acceleration, elevator control and angle of attack are restricted. The most desirable approach velocity can be calculated to give the widest controllable height region. Approach velocity of $1.125 \sim 1.175\ V_s$ gives the widest controllable height region of a middle size turbo-prop aircraft under the proper assumptions.

Using the assumptions that the deviation from the designated approach path obeys the normal distribution, the maximum expected time length to continue the steady state approach flight is calculated. This time length can reasonably be considered to express the margin of safety in approach. When the variance in height from the specified approach path is small, the approach angle should be shallow, and when the variance is large, the angle should be rather steeper in the sense of good safety margin. Restricted to the model aircraft, following is obtained in the limit of ± 0.3 g variational vertical acceleration: If the standard deviation from the specified approach path is 1.0 meter in height, the desirable approach path angle is -2.5 deg., and if the deviation is 3.3 meter, the desirable path angle is -3.2 deg.

It may be concluded that the slope of the glide path of the conventional aircraft ($-2.5 \sim -3.0$ deg.) in ILS is reasonable in view of safety and that, if selected carefully, the location of this glide path to an objective touch down point can be held to the selected point without any adjustment due to the degree of skillfulness of the pilot. This adjustment must be required for more shallow approach path angle.

Acknowledgments

The author is indebted to Associate Professor A. Azuma, University of Tokyo, and Dr. M. Komoda, National Aerospace Laboratory, for their valuable advices and encouragement during this work. Professor A. Azuma also contributed innumerable constructive criticisms for improvement of the presentation.

The numerical calculations were carried out on the computer HITAC 5020F at the Data Processing Center, Institute of Space and Aeronautical Science, University of Tokyo.

Department of Aerodynamics
Institute of Space and Aeronautical Science
University of Tokyo
March 27, 1972

REFERENCES

[1] Innis, R. C.: Factors Limiting the Landing Approach Speed of Airplanes from the Viewpoint of a Pilot. NATO AGARD Report 358 April 1961.

[2] Durand, T. S.: Theory and Simulation of Piloted Longitudinal Control in Carrier Approach. STI Tech. Report No. 130-1 March 1961.

[3] Teper, G. L. & Stapleford, R. L.: An Assessment of the Lateral-Directional Handling Qualities of a Large Aircraft in the Landing Approach. J. Aircraft Vol. 3, No. 3, May–June 1966.

[4] Washicko, L. J.: Application of Approach Speed Criteria Derived from Closed-Loop Pilot Vehicle Systems Analyses to an Ogee Wing Aircraft. NASA CR-579 1966.

[5] Spence, A. & Lean, D.: Some Low Speed Problems of High Speed Aircraft. J. RAS Vol. 66 April 1962.

[6] Kalman, R. E.: Contribution to the Theory of Optimal Control. Bol. Soc. Mat. Mexicana, 1960.

[7] Ellert, F. J. & Merriam III, C. W.: Synthesis of Feedback Control Using Optimization Theory-An Example. IEEE Tr. AC-8 Vol. 2 April 1963.

[8] Friedland, B.: A Technique of Quasi-Optimum Control. Tr. ASME Vol. 88 Jan. 1966.

[9] Kleinman, D. L. et al.: On the Design of Linear Systems with Piecewise-Constant Feedback Gains. IEEE Tr. AC-13 No. 4 Aug. 1968.

[10] Chong, K. L.: Quasi-Optimum Design of an Aircraft Landing Control Systems. J. Aircraft Vol. 7 No. 1 Jan.–Feb. 1970.

[11] Lorenzetti, R. C. et al.: Direct Lift Control for Approach and Landing. AGARD Guidance & Control Panel Meeting S-A-120(L5) AD-686, 081 May 1969.

[12] Komoda, M.: Optimal Partial Power & Vertical Descent Procedure of Multi-Engined Helicopter. Tr. Japan Soc. Aero. Space Sci., Vol. 10 No. 16 1967.

[13] Komoda, M.: An Analytical Method to Predict Ideal H-V Boundary and C.D.P. of Rotorcraft with Special Attention to the Application of Optimalizing Techniques. Joint Symposium on Environmental Effects on VTOL Designs. Preprint No. SW-70-13 Nov. 1970.

[14] Fujii, S. & Sheu, S. Y.: An Application of Stochastic Technique to a Mannual Control Systems. to be published.

[15] Snow, D. R.: Determining Reachable Regions and Optimal Control. Advances in Control Systems 1967 Academic Press.

[16] Lee, E. B. & Markus, L.: Foundations of Optimal Control Theory. John Wiley & Sons 1967.

[17] Sage A,. D.: Optimum Systems Control. Prence-Hall 1968.

[18] Bellman, R. & Dreyfus, S.: Applied Dynamic Programming. Princeton Univ. Press 1962.

[19] Larson, R. E.: Dynamic Programming with Reduced Computational Requirements. IEEE Tr. AC-10 April 1965.

[20] Scharmack, D. K.: An Initial Value Method for Trajectory Optimization Problems. Advances in Control Systems Vol. 5 Academic Press 1967.

[21] Bryson, A. E. & Denham, W. F.: A Steepest-Ascent Method for Solving Optimum Programming Problems. J. Applied Mechanics June 1962.

[22] Pontryagin, L. S. et al.: The Mathematical Theory of Optimal Processes. John Wiley & Sons 1962.

[23] Sinnott, J. F. & Luenberger, D. G.: Solution of Optimal Control Problems by the Method of Conjugate Gradients. IEEE J.A.C.C. 1967.

[24] Denham, W. F. & Bryson, A. E.: Optimal Programming Problems with Inequality Constraints II; Solution by Steepest-Ascent. AIAA J. Vol. 2 No. 1 Jan. 1964.

[25] Lasdon, L. S. et al.: An Interior Penalty Method for Inequality Constrained Optimal Control Problems. IEEE Tr. Vol. AC-12 No. 4 Aug. 1967.

[26] Wolske, C. D. & Flugge Lotz, I.: Minimum Fuel Attitude Control of a Nonlinear

Satellite System with Bounded Control by a Method based on Linear Programming. NASA CR-1450 Oct. 1969.

[27] Kunzi, H. P. et al.: Numerical Methods of Mathematical Optimization with ALGOL and FORTRAN Programs. Translated by Rheinboldt, W. C. et al. Academic Press 1968.

[28] Etkin, B.: Dynamics of Flight, Stability and Control. John Wiley & Sons 1959.

[29] Shayler, J. S.: Radio Guidance Elements of the BLEU Automaitc System for Aircraft. J. British R. E. Jan. 1961.

[30] Fearnside, K.: De Havilland DH121 Trident Part Three-Flight Control System. Aircraft Engineering Jan. 1962.

[31] Koo, H. et al.: A Flight Investigaiton of a STOL Aircraft. NAL TM-146 1968.

[32] Paurez, P. A.: Variation of Landing Distance of Fixed-Wing Aircraft in STOL Operations. J. Aircraft Vol. 2 No. 4 July–Aug. 1965.

[33] Blakelock, J. H.: Automatic Control of Aircraft and Missiles. John Wiley & Sons 1965.

Appendix A Construction of Reference Trcjectory [23]

A-1. Formulation of the Problem

Problem is to determine the controls and trajectories which satisfy the followings:

System Equation

$$\dot{x}=f(x, u) \tag{AP-1}$$

Terminal Condition

$$Dx(t_f)+e=0 \tag{AP-2}$$

where t_f is fixed.

A-2. Discussion in Euclid Space

Let the distance vector from the arbitrary point x^* in Euclid space be δx to the surface

$$Dx+e=0 \tag{AP-3}$$

and let, at the point x, the next relation consist:

$$Dx+e=\phi \tag{AP-4}$$

As δx lies in the perpendicular surface to the

$$Dx+e=0, \tag{AP-5}$$

it can be expressed by using the constant vector c as

$$\delta x=D'c. \tag{AP-6}$$

In other words,

$$D(x+\delta x)+e=Dx+DD'c+e=0 \tag{AP-7}$$

consists. From Eqs. AP-4 and AP-7, we obtain next.

$$\delta x=-D'(DD')^{-1}\phi \tag{AP-8}$$

Thus, we can obtain the amendment vector δx to the surface

$$Dx+e=0. \tag{AP-9}$$

A-3. Extension to Hilbert Space

In Hilbert space, the inner product is defined as

$$(x(t), y(t))=\int_0^{t_f} x'(t)y(t)dt. \tag{AP-10}$$

The variational equation of the system is, if $f\ (x, u)$ is continuously differentiable,

expressed as

$$\delta\dot{x}=f_x(x, u)\delta x+f_u(x, u)\delta u. \tag{AP-11}$$

Let the transition is defined by $\Phi(t, t_0)$ then using the fact that $\delta x=0$, we obtain the next relations:

$$\begin{aligned}\delta x&=\Phi(t,0)\int_0^t\Phi^{-1}(\tau, 0)f_u(\tau)\delta u d\tau\\&=\int_0^t\Phi(t, 0)\Phi(0, \tau)f_u(\tau)\delta u d\tau\\&=\int_0^t\Phi(t, \tau)f_u(\tau)\delta u(\tau)d\tau\end{aligned} \tag{AP-12}$$

Now, so the required terminal condition is

$$Dx(t_f)+e=0, \tag{AP-13}$$

the problem is how to take the amendment control δu to satisfy the above relation. The variation of terminal state by the amendment control δu is

$$\delta x(t_f)=\int_0^{t_f}\Phi(t_f, \tau)f_u(\tau)\delta u(\tau)d\tau \tag{AP-14}$$

Then, let the violating quantities by the control δu be expressed by

$$Dx(t_f)+e=\phi. \tag{AP-15}$$

If the correspondance to Euclid space is taken, the relation of

$$(D, \delta x)=-\phi, \tag{AP-16}$$

or

$$\int_0^{t_f}D\Phi(t_f, \tau)f_u\delta u(\tau)d\tau=-\phi \tag{AP-17}$$

is anticipated. Using the transformation of

$$\tilde{D}=D\Phi(t_f, \tau)f_u, \tag{AP-18}$$

Eq. AP-17 becomes to

$$(\tilde{D}, \delta u)=-\phi \tag{AP-19}$$

On the other hand, from the correspondance to Euclid space, we can assume the relation of

$$\delta u=\tilde{D}'c. \tag{AP-20}$$

From Eq. AP-19,

$$\int_0^{t_f} \tilde{D}\tilde{D}'c dt = -\phi \tag{AP-21}$$

or

$$c = -\left[\int_0^{t_f} \tilde{D}\tilde{D}' dt\right]^{-1}\phi = -\left[(\tilde{D}, \tilde{D}')\right]^{-1}\phi \tag{AP-22}$$

can be obtained. This corresponds to the Eq. AP–8 in the discussion in Euclid space. Substituting this relation to Eq. AP–20 we can get the following:

$$\delta u = -\tilde{D}'\left[\int_0^{t_f} \tilde{D}\tilde{D}' dt\right]^{-1}\phi \tag{AP-23}$$

This is the amendment control to be taken.